The Cryosphere, 20, 2257–2277, 2026
https://doi.org/10.5194/tc-20-2257-2026

The Cryosphere Open Access EGU

Glacial decline next to stable permafrost in the Dry Andes? Vertical glacier surface changes and rock glacier kinematics based on Pléiades imagery (Rodeo basin, 2019–2025)

Melanie Stammler[1], Jan Blöthe[2], Diego Cusicanqui[3], Simon Ebert[2,a], Rainer Bell[1], Xavier Bodin[4], and Lothar Schrott[1]

[1]Department of Geography, University of Bonn, Bonn, 53115, Germany
[2]Faculty of Environment and Natural Resources, University of Freiburg, Freiburg, 79104, Germany
[3]Institut des Sciences de la Terre (ISTerre) CNES, CNRS, IRD, Univ. Grenoble Alpes, Grenoble, 38000, France
[4]Laboratoire EDYTEM, CNRS/Université Savoie Mont Blanc, Le Bourget du Lac, 73370, France
[a]current address: Department of Earth and Planetary Sciences, ETH Zurich, Zurich, 8092, Switzerland

Correspondence: Melanie Stammler (stammler@uni-bonn.de)

Received: 20 September 2025 – Discussion started: 17 November 2025
Revised: 3 March 2026 – Accepted: 26 March 2026 – Published: 21 April 2026

Abstract. The presence and volume of high-mountain cryospheric features are drastically affected by rising air temperatures – on global scale. In the Dry Andes, precipitation is extremely scarce, shifting the hydrological significance towards the solid water storages, glaciers and ground ice. While glaciers decrease in surface area and volume, periglacially stored waters, e.g., in rock glaciers, react more retarded to atmospheric forcing, potentially buffering future water availability. Despite rising air temperatures, recent studies suggest stable permafrost conditions in the Dry Andes based on borehole investigation and rock glacier kinematics for the last decade. This apparent stability may partly reflect the extreme aridity conditions, limit snow insulation and liquid-water input, thereby damping inter-annual variability in ground thermal conditions and associated changes in rock glacier creep.

We investigate vertical surface changes of 19 glaciers, three debris-covered glaciers and 59 rock glaciers in the Rodeo basin (Dry Andes, Argentina) for the time period 2019–2025. Further, we calculate rock glacier velocities for 47 of the 59 rock glaciers for which we have data for all time periods. Photogrammetric principles are followed using (tri)stereo, panchromatic Pléiades imagery to generate projected optical imagery and DEMs in Ames Stereo Pipeline. Resulting DEMs are co-registered prior to DEM differencing for vertical surface change calculation. To derive rock glacier velocities, a feature tracking approach is applied to panchromatic Pléiades orthoimagery.

We detect glacier surface lowering of up to −8.99 m (total change, 2019–2025) and dominantly annual surface lowering for all glaciers investigated. Vertical surface lowering on debris-covered glaciers falls well below the magnitude of glaciers, but is higher than for rock glaciers – the latter not exceeding a decimetre. Average rock glacier velocities fall between 0.28 and 0.82 m yr^{-1} (Levels of Detection, LoDs: ±0.16, ±0.61). The presence of highest magnitude of horizontal velocities is different between rock glaciers, with highest horizontal velocities partially reached in the upper or lower part of the rock glacier surface. Across the 47 rock glaciers investigated, no regional trend of increasing velocities is found.

In conclusion, the declining glacial domain contrasts with unchanged rock glacier velocities which elucidate stable permafrost conditions. We infer a delayed reaction of the periglacial domain to the rising temperatures that lead to the surface lowering of glaciers and highlight the need for ongoing, long(er)-time surface change monitoring in this crucial, dynamic point in time.

Published by Copernicus Publications on behalf of the European Geosciences Union.

1 Introduction

The cryosphere of the Dry Andes of Argentina is an important water reservoir, buffering periods of drought (Dussaillant et al., 2019) and sustaining water use by meltwater contribution to river runoff (Ferri et al., 2020; Masiokas et al., 2020; Pitte et al., 2022; Schrott and Götz, 2013). All cryospheric components in this region are exposed to increasing temperatures (Pabón-Caicedo et al., 2020; Pitte et al., 2022) and high variability in magnitude and pattern of precipitation. Compared to glacially stored waters, periglacially stored waters express a longer and extended response time to climatic changes (Arenson et al., 2022). Particularly in arid regions, the detection and quantification of such solid water storages, e.g., ice lenses in permafrost settings, is crucial, with their hydrological relevance increasing in the future (Arenson et al., 2022).

Glaciers in the Dry Andes of Argentina decrease in surface area and volume (Dussaillant et al., 2019; Masiokas et al., 2020; Pitte et al., 2022; Hugonnet et al., 2021), with sublimation strongly affecting glacial ice loss (Ayala et al., 2016; Réveillet et al., 2020). Mass balances for Agua Negra Glacier, located in the study area, reach −3.67 m water equivalent (w.e.) (2020–2021) based on the glaciological method (Pitte et al., 2022). Independent of density parameters, surface lowering presents a first indication of glacier ice loss. For debris-covered glaciers, the debris cover thickness strongly affects the magnitude of ice volume loss (Ferri et al., 2020), thus, the magnitude of vertical surface change. While ablation patterns are heterogeneous, particularly in regions with supraglacial ponds and/or ice cliffs (Ayala et al., 2025; Bodin et al., 2010; Falaschi et al., 2021), thinning (Ayala et al., 2025; Lenzano et al., 2016) or thickening rather than terminus recession is reported as climate response of debris-covered glaciers (Falaschi et al., 2021). In terms of their hydrological significance, debris-covered glaciers are reported to contribute to streamflow in a magnitude similar to glaciers (Ayala et al., 2016).

(Dis)continuous permafrost conditions are present in approximately 11 000 km^2 of the Dry Andes (17°30′ to 35° S, Borsdorf and Stadel, 2013), based on a Permafrost Zonation Index above 0.5 (Gruber, 2012). They are present across a high variability of periglacial landforms, spanning block- and talus slopes (Köhler et al., 2025), protalus ramparts, and rock glaciers (Halla et al., 2021; Robson et al., 2022; Stammler et al., 2025a). Recent studies suggest stable permafrost conditions in the Dry Andes for the last decade based on borehole ground temperature measurements (Koenig et al., 2025) and the monitoring of rock glacier kinematics (Blöthe et al., 2024; Stammler et al., 2025a).

Rock glaciers, consisting of debris, air and ice, are characteristic of permafrost environments (Barsch, 1992; RGIK, 2022). Their surface kinematics comprise the vertical and horizontal component and are descriptive of the rock glaciers' mechanical behaviour evident as internal deformation processes and/or surface motion (Hu et al., 2025). Surface movement in horizontal direction, termed rock glacier velocity (RGV), was recently incorporated into the essential climate variable permafrost and is, while focusing on continuous and comparable monitoring, indicative for kinematic changes within the rock glacier body (Hu et al., 2025; RGIK, 2023). Rock glacier monitoring efforts in the Andes are scarce (Hu et al., 2025), with few studies on rock glacier kinematics (Blöthe et al., 2021, 2024; Cusicanqui et al., 2025; Halla et al., 2021; Robson et al., 2022; Stammler et al., 2025a; Strozzi et al., 2020; Villarroel et al., 2018; Villarroel and Forte, 2020; Villarroel et al., 2022). Studies on vertical surface changes on rock glaciers are even more rare, with vertical surface changes reported to be minimal (Halla et al., 2021; Robson et al., 2022; Vivero and Lambiel, 2024).

Given the rock glaciers' permafrost indication and hydrological significance, the analysis of rock glaciers can greatly contribute to interdisciplinary studies, for example, focusing on a catchment's hydrology. However, rock glacier studies often focus on chosen single rock glaciers. Moreover, only few studies investigate changes in the glacial and periglacial domains (Bodin et al., 2010; Cusicanqui et al., 2023), even fewer on a catchment scale (Falaschi et al., 2025; Robson et al., 2022), providing a comprehensive picture on current changes in the high-mountain cryosphere.

Satellite-based photogrammetry, by now a standard method applied for RGV monitoring (Hu et al., 2025), enables an increased spatial extent and an access- and weather conditions independent study compared to field-based studies. Photogrammetric processing software allows for the generation of digital elevation models (DEMs) based on an overlap of satellite imagery. While DEM differencing of correctly co-registered DEMs enables the calculation of vertical surface changes across landforms, feature tracking on projected, panchromatic imagery allows for the calculation of the horizontal component. (Tri)stereo panchromatic Pléiades imagery has been used for change detection in the field of geosciences (Bagnardi et al., 2016; Beraud et al., 2023; Berthier et al., 2024), often with a focus on glaciology.

In this paper, we investigate the current state of the cryosphere in Rodeo basin (Dry Andes of Argentina, 30° S and 69° W) by analysing vertical surface change on 19 glaciers, three debris-covered glaciers, and 59 rock glaciers, as well as horizontal velocity on, due to data coverage, 47 of the 59 rock glaciers for 2019–2025 based on (tri)stereo panchromatic Pléiades imagery. This means that we focus on vertical surface change across all cryospheric landforms but in particular on horizontal velocities of rock glaciers in the Rodeo basin. With the study we intent to increase the knowledge on the high-Andean cryosphere in a changing climate, address the above-described gap of combined and catchment wide studies for the glacial and periglacial domains, and contribute to the understanding of the state of permafrost in the arid environment of the Dry Andes. We address the following research questions:

- Which vertical surface changes can be observed on glaciers and debris-covered glaciers and how do these changes compare to vertical surface changes of the rock glaciers in the study area?
- Which vertical and horizontal rock glacier surface changes can be observed across the Rodeo basin and what do these changes imply for the local permafrost conditions?
- What are the advantages and limitations of a Pléiades-based surface change monitoring of glaciers, debris-covered glaciers and rock glaciers in the Dry Andes?

By simultaneously addressing the glacial and periglacial domains as well as increasing the spatial scale of our surface change monitoring to a catchment resolution, we foresee to contribute to a better understanding of the current status of the regional solid water storages in the Dry Andes at a, given rising air temperatures, crucial moment in time.

2 Study Area

The Rodeo basin is located in the Dry Andes, in the Western part of the San Juan Province/Argentina (30° S and 69° W), Fig. 1. The high Andean basin hosts 19 glaciers, three debris-covered glaciers, and 59 rock glaciers (IANIGLA-CONICET, 2018), representative of a region-typical (peri)glacial landform distribution with few glaciers located at high elevations, dominated by a large number of periglacial landforms (Halla et al., 2021; Köhler et al., 2025), Fig. 1A. With a basin size of 1315.7 km^2, the basin's upper part is strongly impacted by the Cordillera Principal in the west ($<$ 6947.5 m a.s.l.) and is underlain by permafrost, with continuous permafrost present above 5000 m a.s.l. (Gruber, 2012; Halla et al., 2021; Schrott, 1996). Most of the basin's runoff discharges to the reservoir Cuesta del Viento located in the inter-mountainous basin between the Cordillera Principal and the Cordillera Frontal (Esper Angillieri, 2017) near Rodeo, Fig. 1B, at approximately 1500 m a.s.l. Glaciers in the basin are larger in size than rock glaciers, Fig. 2B, are located at higher elevation and are characterized by higher surface slopes, Fig. 1C. As a consequence of valley structures and the rock glaciers' location closer to the valley bottom, they are most often oriented east or south-east, rarely north or west. Characterized by extremely low mean annual precipitation ($\sim$ 250 mm), a mean annual air temperature of -4.9 °C (1961–1990, ERA5) and constant high solar radiation intensities (Lliboutry et al., 1998; Schrott, 1994), solid water storages in the form of glacial or ground ice and their meltwaters are essential to river runoff (Dussaillant et al., 2019; Masiokas et al., 2020), with the relative hydrological significance of periglacially stored ice increased in the future (Arenson et al., 2022). According to Caro et al. (2024), the glaciological zone which includes, e.g., Tapado glacier located in ca. 10 km distance west of Agua Negra Glacier in the Chilean Andes, is characterized by the highest vulnerability to glacier runoff scarcity across the Andes. Research on the periglacial domain of the study area has focused on Agua Negra catchment which is part of the upper Rodeo basin (Halla et al., 2021; Köhler et al., 2025).

3 Data and Methods

We analyse interannual vertical surface change on 19 glaciers, three debris-covered glaciers and 59 rock glaciers in the Dry Andes of Argentina for 2019–2025. Further, we investigate horizontal velocities on 47 of the 59 rock glaciers consistently monitored for 2019–2025. We use (tri)stereo, panchromatic Pléiades imagery acquisitions for the austral summers of 2019, 2022, 2023, 2024 and 2025 for the generation of Pléiades-based DEMs and consequent DEMs of Difference (DoDs) for vertical change detection on all landforms. For rock glacier horizontal velocities, we conduct feature tracking on projected panchromatic Pléiades imagery.

3.1 National Inventory of Glaciers (Argentina)

Glaciers, debris-covered glaciers, rock glaciers (active/inactive) and perennial snowfields across the Argentinean Andes and South-Atlantic islands cover an area of 8484 km^2 and are documented in the National Inventory of Glaciers conducted by the Argentine Institute for Snow, Ice and Environmental Sciences (IANIGLA-CONICET) in collaboration with the Argentine Ministry of the Environment and Sustainable Development (Zalazar et al., 2017). With the aim of preserving glaciers and the periglacial environment, the dataset was established based on satellite imagery and ground-truthing as requirement of the law on Minimum Standards for the Preservation of Glaciers and the Periglacial Environment (span. Régimen de Presupuestos Mínimos para la Preservación de los Glaciares y del Ambiente Periglacial) (ibid.).

We rely on the National Inventory of Glaciers for glacial and periglacial feature boundaries in our study area and conduct our vertical surface changes and horizontal velocity analysis within these boundaries. For our analysis, we treat rock glaciers indifferent of their mapped state of activity allowing us to rely on our measured horizontal velocity quantification rather than the visual interpretation of surface features as conducted during the establishment of the inventory (Zalazar et al., 2017, 2020).

3.2 3.2 Pléiades Imagery Acquisitions and Processing

The Pléiades 1A and 1B satellites were launched on 17 December 2011 and 2 December 2012 respectively. With a sun-synchronous orbit type and repeat cycle 26 d, they offer panchromatic (resolution 0.5 m) and multispectral (resolution 2 m) imagery in stereo and tristereo mode (ASTRIUM, 2012). Achieving the (tri)stereo cover during one pass over the area, a homogeneous product which allows for most pre-

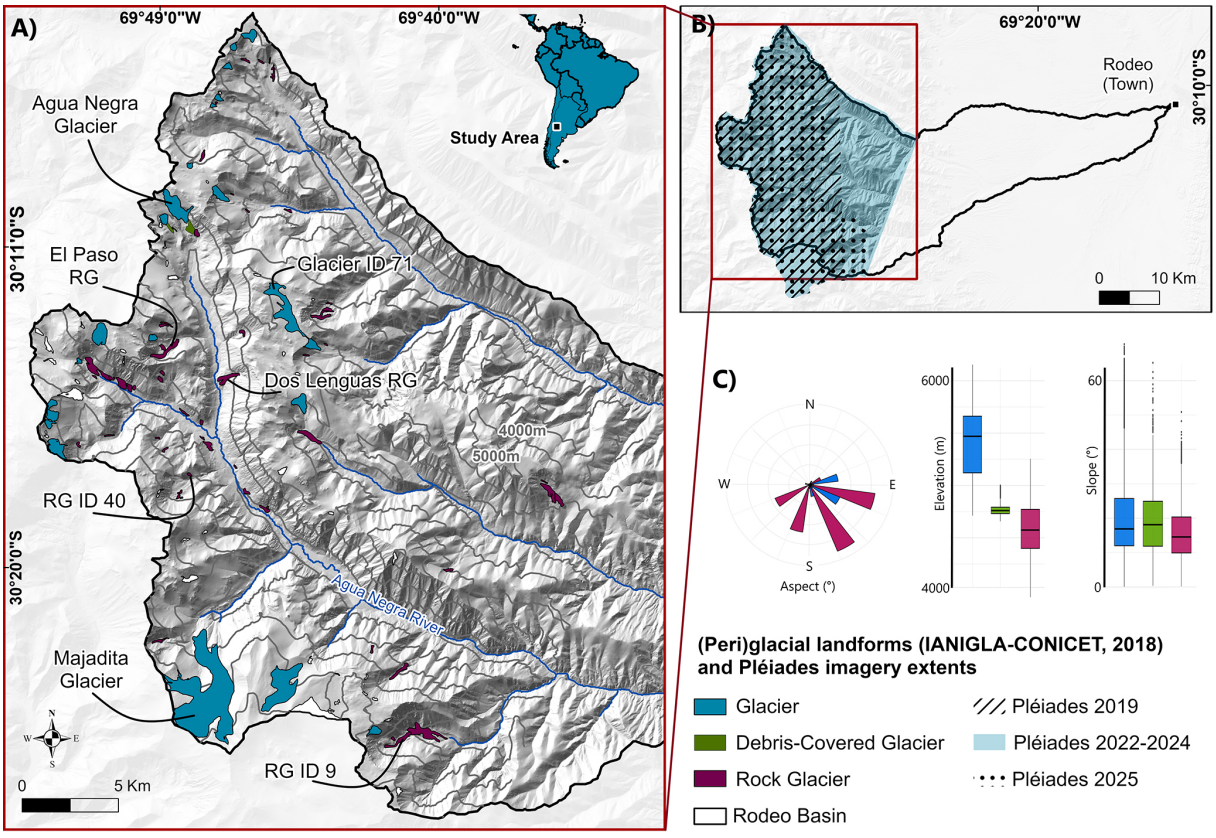

Figure 1. **(A)** Distribution of glaciers, debris-covered glaciers and rock glaciers as mapped by IANIGLA-CONICET (2018) in the upper part of Rodeo basin. All landforms labelled here are detailed in consequent figures. **(B)** Rodeo basin including the extents of the Pléiades imagery acquisitions (cf. Fig. S1 in the Supplement). **(C)** Aspect, elevation and slope characteristics of the (peri)glacial landforms of the study area, calculated from a 10 m DEM (based on the 2022 Pléiades data, Table 1) and its derivatives. Colour-scale for landform type applies to all panels.

Table 1. Acquisition dates and characteristics of the four (tri)stereo panchromatic Pléiades datasets. All dates are provided as dd.mm.yy. In the remaining paper, the overlapping image tiles acquired at different acquisition dates are referred to as top (T), bottom (B) and right (R) tiles. For the location of the three tiles, see Fig. S1. B / H ratios are comparable with other studies, e.g., Beraud et al. (2023).

	2019	2022	2023	2024	2025
Image Acquisition Date(s) and Tile Locations (T, B, R)	17.03.19	14.02.22 (T) 22.02.22 (B) 15.02.22 (R)	13.02.23 (T) 20.02.23 (B) 14.02.23 (R)	12.02.24 (T) 19.02.24 (B) 09.03.24 (R)	02.03.25 (T) 03.03.25 (B) –
Geometry	stereo	tristereo			
B / H	0.4	0.3–0.5			
Max Inc. Angle		$< 20°$			
Max Cloud Cover		$< 5\,\%$			

cise DEMs to be generated is acquired despite the challenging terrain of the Andes – and allows for a suitable base-to-height (B / H) ratio. In contrast to radar imagery, the optical signal does not penetrate snow and ice, increasing suitability for cryospheric surface change detection (Berthier et al., 2014). All Pléiades data used in this study were tasked for austral summers, in stereo (2019) or tristereo (2022–2025) mode and processing level 1 corresponding to the primary product (ASTRIUM, 2012), Table 1.

We process all Pléiades (tri)stereo pairs automatically using Ames Stereo Pipeline (ASP) software (Beyer et al., 2018). Processing is conducted without ground control

points (GCPs) relying on rational polynomial coefficients (RPCs). We follow Berthier et al. (2024) and Cusicanqui et al. (2025) in using a STRM DEM as seed DEM during stereo processing and a semi-global matching strategy. Here, either both stereo acquisitions or both pairs of the tri-stereo triplet are included. As a result, we generate DEMs at 1 m resolution. Given the data quality we do not fill gaps and proceed without correcting for sensor undulations.

3.3 DGNSS measurements for validation

We conduct 78 repeated Differential Global Navigation Satellite System (DGNSS) measurements on Dos Lenguas and El Paso rock glaciers as well in the Agua Negra Glacier forefield using Trimble DGNSS equipment (R8 base, R2s rover, TSC3 handheld, RTK), Table 2. Located on the landforms as well as surrounding terrain, the measurements are conducted in at least 2 consecutive years in the austral summers of 2022, 2023 and 2024; within maximum 2 consecutive days. Measured point locations are marked on flat surfaces of selected large boulders (> 2 m). The coordinates of the base stations are 424101.83, 6654084.621, 4247.137 m for Dos Lenguas rock glacier; 422350.62, 6655630.667, 4723.248 m for El Paso rock glacier and 422783.389, 6661216.068, 4726.973 m for the Agua Negra Glacier forefield – all provided in WGS 84 UTM zone 19S. DGNSS measurements on Dos Lenguas rock glacier have been used for validation and georeferencing (Stammler et al., 2024, 2025a) and are published in Stammler et al. (2025b). We publish the additional DGNSS measurements used in this study in the paper-accompanying dataset (Stammler et al., 2026).

3.4 Vertical surface change by DEMs of Difference

We buffer the inventoried landforms and generate rectangular bounding boxes, resulting in bounding boxes with minimum 500 m distance to each of the (debris-covered) glacier and rock glacier polygons to clip our Pléiades-based DEMs. Consequently, we co-register the younger to the older clipped DEMs following Nuth and Kääb (2011) in Demcoreg (Shean et al., 2016), while masking the cryospheric landforms based on the National Inventory of Glaciers (IANIGLA-CONICET, 2018). Single Pléiades tiles are processed separately to prevent distortion from mosaicking. If available for both acquisitions, each tile is co-registered respectively, e.g., 2023T to 2022T, 2023B to 2022B, 2023R to 2022R. For acquisitions with different extents and/or number of tiles, co-registration is only possible where data is available and is conducted as, e.g., 2022T to 2019, 2022B to 2019, 2022R to 2019. Co-registering clipped rasters allows for an adaption to the local setting of each landform, preventing larger distortion patterns to imprint on the DEM-based analysis while reducing processing times. Further, it enables temporal and spatial investigation of the x, y, z correction factors used during co-registration.

For the calculation of the LoDs of our vertical surface changes, we extract vertical surface change at 1000 random points distributed outside and in vicinity of each landform polygon and derive their median. Terrain outside the landform polygons is assumed to be predominantly stable. Having controlled vertical surface change in the areas outside the landform surfaces during co-registration, we directly accept the medians as LoDs. For vertical surface change quantification by DEM differencing, we subtract the co-registered newer DEMs from the original older DEMs. Depending on the figure, vertical surface change of the cryospheric landforms in the Rodeo basin is compared as total change (sum of annual median change, Fig. 2A) or as vertical surface change normalized to full years, both calculated as median for the landforms' surfaces, Figs. 2B–D and 5A. Rock glaciers are attributed positive when vertical surface change plus and minus the LoD are above zero, and negative when both are below zero. Further, we derive elevation and slope from the Pléiades DEMs, all at a resolution of 1 m.

3.5 Horizontal velocity by feature tracking

We use the projected panchromatic imagery at 0.5 m resolution to conduct feature tracking on all rock glaciers for which we have data for all time periods (47 out of 59) following the approach by Schwalbe and Maas (2017) which matches image patches between orthoimages with two different time stamps by applying cross-correlation for an estimation of a pixel-precise shift, and a least-squares matching for the achievement of sub-pixel accuracies. Originally implemented in the Environmental Motion Tracking (EMT) software, we adapt this approach to semi-automatically process a large quantity of rasters in python (Ebert and Rehn, 2026). For our stereo dataset (2019), we select the first image of the pair with a view angle tilted towards south. For the tristereo datasets (2022–2025), we select the second image of the triplet which is closest to nadir view (90°).

Similar to the DEMs, we clip the panchromatic orthoimages by our bounding boxes prior to feature tracking. After conducting an affine transformation for offset correction, identifiable pixels are tracked on the landform surface (no front and side slopes) using a set of equally, 5 m spaced points – leading to a 5 m spatial resolution of the calculated velocities. This approach benefits from using grey-scaled input which is independent of light conditions (Dall'Asta et al., 2017; Fleischer et al., 2021). To reduce the impact of the polygon boundaries as included in the National Inventory of Glaciers (IANIGLA-CONICET, 2018) on the feature tracking outcome, we apply a 200 m buffer on all polygons to determine the reference area used for aligning the images while we use a buffer of 50 m around the polygons for the actual image tracking. Horizontal rock glacier velocity is presented normalized to full years. To enable the comparison of horizontal velocity values with varying LoDs, we calcu-

Table 2. Acquisition dates and characteristics of our DGNSS measurements, used for validation purposes. For rock glaciers, the number of points is split in onsite and offsite the landforms' surface. The DGNSS measurements of Dos Lenguas rock glacier are published in Stammler et al. (2025b). All other DGNSS data are published in Stammler et al. (2026).

	Dos Lenguas RG	El Paso RG	AN forefield
Acquisition Dates (dd.mm.yy)	17.03.22–21.03.22 16.01.23–12.02.23 10.02.24–12.02.24	– 01.02.23–02.02.23 14.02.24	08.03.22 17.01.23 26.02.24
No. of points	21 (8/13)	36 (26/10)	21
Mean accuracy H/V (in m)	0.017/0.028	0.036/0.076	0.018/0.041

H/V: horizontal/vertical. RG = rock glacier, AN forefield = Agua Negra glacier forefield.

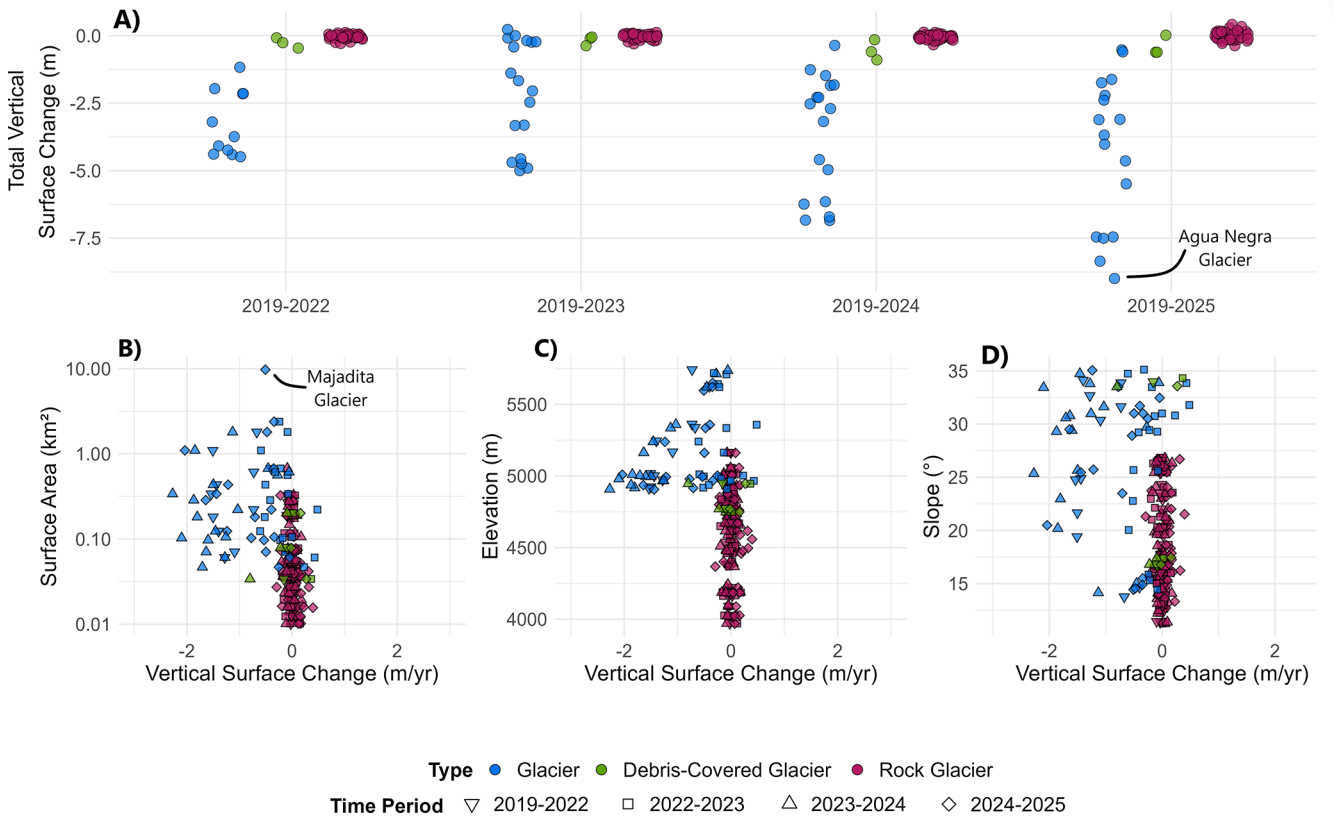

Figure 2. **(A)** Total vertical surface change for glaciers, debris-covered glaciers and rock glaciers for 2019–2025. Calculated as the sum of the median annual vertical surface change per landform polygon and within the landform surfaces (e.g., no rock glacier fronts) based on DEM differencing between clipped, co-registered Pléiades DEMs. The number of the landforms investigated depends on the extent of the Pléiades acquisitions, cf. Fig. 1B. Median annual vertical surface change normalized to full years and its concurrence with the landform surface area **(B)**, with elevation **(C)** and slope **(D)**. Elevation and slope are derived from the Pléiades-DEM at the beginning of the time period, e.g., 2019 for the 2019–2022 period. Symbol types correspond to the time periods as introduced in the legend. For the location of Agua Negra and Majadita Glaciers, see Fig. 1A.

late the median exceedance from the corresponding LoD for each rock glacier and time step, Fig. 7A.

Similar to the calculation of the LoDs for vertical surface changes, surface motion is tracked at 1000 randomly distributed points located outside of the landform surface for the calculation of the LoDs of the horizontal rock glacier velocities. We accept the median of the feature tracking results at these 1000 random points as LoD. Selecting the median serves as a precautionary measure against singular of the randomly distributed points coincidentally placed on moving objects.

We track the residuals of the affine transformation during our feature tracking approach to develop a criterion for the quality of the image alignment, which directly affects the feature tracking results. We detect the correlation of these residues in x, y space and use low correlation coefficients (0 to 0.5) as indication of a high-quality feature tracking and high correlation coefficients (0.5 to 1) as indication of a poorer feature tracking quality. The implementation of the correlation coefficient of the residues that arise during feature tracking as a quality control is based on the hypothesis that high correlation is indicative of a technical error, e.g., an image distortion, while true residues are expected to be independently distributed. We include this quality criterium as a metric and as categories.

4 Results

4.1 Co-registration, DEM differencing and feature tracking accuracies

The area's aridity and extremely limited cloud and vegetation cover yield perfectly suitable conditions for change analysis with remotely sensed optical imagery, such as Pléiades imagery. The summer conditions with very scarce and, if present, non-persistent snow coverage allow for largely uncovered terrain suitable for co-registration, Fig. S1. For co-registration, X correction factors are of least magnitude in median through time, while Z correction factors are of highest, Table 3. A comparison of the T, B, and R tiles indicates no consistent pattern of spatial differences in co-registration factors. All correction factors used during co-registration are independent of the landform type, Fig. S2.

Vertical surface changes as extracted at 1000 randomly distributed points surrounding the landform polygons are independent of the landform type and time period and correspond to the respective LoD of our vertical surface changes, Table 4. They vary between ± 0.1 and $\pm 10\,\mathrm{cm\,yr^{-1}}$ when compared as median for all landforms of each landform type (glaciers, debris-covered glaciers, rock glaciers). Vertical change LoDs are lower than the LoDs calculated for horizontal velocities. Median horizontal velocities at 1000 randomly placed points in vicinity of the rock glacier surfaces range between ± 16 and $\pm 61\,\mathrm{cm\,yr^{-1}}$ and represent our LoDs for horizontal velocities. The calculated LoDs for horizontal velocities are low for the 2019–2022 and 2023–2024 time periods, compared to 2022–2023 and 2024–2025.

Correlation factors of the residues arising during our feature tracking approach range in median over time for the selected rock glaciers between 0.27 (ID44) and 0.64 (ID39), Table 5. This is representative for all polygons, with the least and highest correlation being 0.12 (ID25) and 0.66 (ID47), Table S2. In total, 45 of the 57 polygons are characterized by low correlation coefficients of the residues (0 to 0.5), with 12 polygons exceeding a coefficient of 0.5 but none reaching a coefficient of 0.7. In median and independent of the different rock glacier polygons, the time period 2023–2024 is characterized by least correlation of the residues both for the selected rock glaciers (2023–2024: 0.26) as well as all polygons (2023–2024: 0.28). Thus, three out of the four time periods are characterized by low correlation coefficients with one exceeding a coefficient of 0.5 but remaining below 0.6, both for the selection as well as for all polygons.

4.2 Pléiades-based vertical surface changes for (debris-covered) glaciers and rock glaciers in the Rodeo Basin

Vertical surface change across the cryospheric landforms in the Rodeo basin is highest in magnitude for glaciers, second highest for debris-covered glaciers and least for rock glaciers – independent of the time period, Fig. 2A. Calculated LoDs are very low compared to the vertical surface changes on glaciers, low compared to debris-covered glaciers and vertically dynamic rock glaciers, and high compared to rock glaciers with minimal vertical surface change when calculated as median for the landforms' surface, Table 4.

All glaciers monitored in our study are characterized by negative vertical surface changes, leading to negative total vertical surface change increasing in magnitude, Fig. 2A. Total vertical surface change is of highest magnitude for Agua Negra Glacier ($1.09\,\mathrm{km^2}$, 5012 m a.s.l., 2nd largest glacier in the study area) amounting to a vertical elevation change in median for the glacier surface of -8.99 m for 2019–2025, detected with a LoD of $\pm 0.11\,\mathrm{m\,yr^{-1}}$. Increase in time-normalized annual vertical surface change is not linear, highest for 2023-20-24 ($-1.50\,\mathrm{m\,yr^{-1}}$, LoD $\pm\,0.01\,\mathrm{m\,yr^{-1}}$) and lowest for 2022–2023 ($-0.20\,\mathrm{m\,yr^{-1}}$, LoD $\pm\,0.001\,\mathrm{m\,yr^{-1}}$), Table 4. Time-normalized annual vertical surface changes of Agua Negra Glacier are higher than of the largest glacier monitored with our Pléiades imagery for the full time period (ID71, $1.80\,\mathrm{km^2}$, 5335.5 m a.s.l.), Table 6. In general, smaller glaciers are characterized by higher time-normalized median vertical surface change than large glaciers, Fig. 2B. Further, vertical surface change is highest in magnitude for glaciers at lower elevations, Fig. 2C, and independent of slope, Fig. 2D.

Only three debris-covered glaciers are present in the Rodeo basin with median vertical surface changes up to $-22\,\mathrm{cm\,yr^{-1}}$, detected with a LoD of ± 10 cm, Table 6.

Rock glacier vertical surface change is minimal on Dos Lenguas and El Paso rock glaciers. This is representative for all rock glaciers monitored, Fig. 2A and Table 4. Rock glacier vertical surface changes are not correlated with median elevation or slope, Fig. 2C-D. However, rock glaciers in the Rodeo basin are characterized by an interannual variability of vertical surface change, with 47 rock glaciers alternating at least once between positive and negative median annual surface change between the observed time episodes (6 always negative, 4 always positive).

Table 3. Co-registration corrections in x, y, and z direction based on the approach by Nuth and Kääb (2011) as applied in Demcoreg (Shean et al., 2016). Shown as median of all co-registration factors (m) of the 81 clipped DEMs (number of landforms = 81). For all co-registration factors, see Table S1 in the Supplement.

	Shift in x (m)			Shift in y (m)			Shift in z (m)			Median (m)
	T	B	R	T	B	R	T	B	R	
2019–2022	−0.16	0.2	−0.18	0.24	0.23	0.44	1.22	1.04	2.62	0.24
2022–2023	−0.2	−0.08	0.00	−0.08	−0.01	−0.32	0.59	−0.56	−0.90	−0.08
2023–2024	0.26	−0.06	0.20	−0.47	−0.12	0.34	−0.76	0.81	0.58	0.2
2024–2025	0.05	−0.16	–	0.59	0.07	–	0.05	−1.55	–	0.05
Median (m)	−0.06	−0.07	0	0.08	0.03	0.34	0.32	0.13	0.58	

Table 4. Vertical surface change ($m\,yr^{-1}$) on (debris-covered) glaciers as well as vertical surface change and horizontal velocities ($m\,yr^{-1}$) on rock glaciers shown as medians for all landforms within each category. LoDs for vertical surface change and horizontal velocities are based on the median of surface change at 1000 randomly distributed points in vicinity of the landforms, shown here as medians per landform category. For rock glacier velocities, we consider only surface change exceeding the respective LoD.

	Glaciers			Debris-c. Glaciers			Rock Glaciers					
	VCh	LoD	n	VCh	LoD	n	VCh	LoD	n	HVe	LoD	n
2019–2022	−1.28	±0.01	11	−0.09	±0.08	3	−0.01	±0.03	48	0.28	±0.16	38
2022–2023	−0.20	±0.001	18	0.02	±0.01	3	0.004	±0.003	59	0.64	±0.52	25
2023–2024	−1.50	±0.01	17	−0.22	±0.10	3	−0.01	±0.004	59	0.46	±0.17	28
2024–2025	−0.51	±0.001	17	0.16	±0.02	3	0.07	±0.001	54	0.82	±0.61	33

VCh = Vertical surface change, HVe = Horizontal velocity, n = number of landforms, depending on the spatial extent of the image acquisition.

Spatially, time-normalized vertical surface changes on Agua Negra Glacier are heterogeneously present with highest magnitudes on its west side and towards the glacier tongue, Fig. 3A. Vertical changes on the largest glacier (ID 71) are also heterogeneously present, with highest magnitudes reached in the centre and southern part, Fig. 3B. The glacier located next to El Paso rock glacier exhibits vertical surface changes particularly in its centre, Fig. 3C. Rock glacier vertical surface changes are spatially heterogeneous and often follow a ridge- and furrow morphology with alternating positive and negative areas, Fig. 3D. Rock glacier fronts are characterized by a coherent positive vertical surface change, Fig. 3C–D. For vertical surface changes of all monitored cryospheric landforms, see Fig. 3E.

4.3 Pléiades-based rock glacier velocities for Rodeo Basin in space and time

Rock glaciers in the Rodeo basin exhibit differences in the magnitude of their horizontal velocity in space with median rock glacier surface velocities being heterogeneously present in the Rodeo basin, Fig. 4. Their LoDs are independent of a rock glacier's location, size, and horizontal velocity. Out of the 47 rock glaciers, 1 rock glacier exceeds median velocities of $> 1.25\,m\,yr^{-1}$ for the time period 2019–2025 (Dos Lenguas rock glacier), while 7 rock glaciers fall between 1 and $1.25\,m\,yr^{-1}$ (e.g., El Paso rock glacier), and 14 fall in the classes between 0.75–1 and 0.5–0.75 $m\,yr^{-1}$, respectively. The LoD exceedance of median rock glacier surface velocities based on all rock glaciers varies between 0.12 and $0.29\,m\,yr^{-1}$, Table 4 (HVe minus respective LoD), non-linear in time.

Correlation coefficients support that larger rock glaciers are faster than those characterized by a smaller surface area, that rock glaciers located at higher location are faster than rock glaciers located at lower elevation, and that smaller rock glaciers are characterized by higher slope than larger rock glaciers. For all correlation coefficients, see Table S3. Larger rock glaciers ($> 0.1\,km^2$) in their vast majority exhibit velocities above $0.25\,m\,yr^{-1}$ in all time periods, while smaller rock glaciers ($< 0.1\,km^2$) are characterized by various horizontal velocities from 0.0 to $1.23\,m\,yr^{-1}$, Fig. 5A. Rock glaciers located at elevations below 4100 m a.s.l. do not exceed horizontal velocities of $0.25\,m\,yr^{-1}$, while all rock glaciers located above 4300 m a.s.l. exceed horizontal velocities of $0.09\,m\,yr^{-1}$ and reach up to $1.38\,m\,yr^{-1}$, Fig. 5B. Slope and rock glacier velocity are not correlated, Fig. 5C, and variability of median vertical change is dependent on the time period – with 2022–2023 characterized by more negative and 2023–2024 by more positive median vertical surface changes, Fig. 5D. For a full visualization of the concurrence of elevation and slope separated by time periods and colour-

Table 5. Correlation coefficients for residues arising during the affine transformation of our feature tracking approach on selected rock glaciers (RG). Rock glaciers are selected based on their size and speed (large $> 0.1\,km^2$, fast $> 0.2\,m\,yr^{-1}$). For a full list of correlation coefficients, see Table S2. We treat low correlation coefficients (0 to 0.5) as criterium for a high quality of the feature tracking approach and higher correlation coefficients (0.5 to 1) as a poorer quality of the feature tracking approach, cf. 3.5.

	Large and fast RG			Small and fast RG			Small and slow RG			Median (m)
	ID4	ID5	ID9	ID24	ID40	ID50	ID35	ID39	ID44	
2019–2022	0.64	0.62	0.21	0.79	0.55	0.32	0.44	0.74	0.42	0.55
2022–2023	0.20	0.34	0.45	0.22	0.72	0.11	0.85	0.66	0.80	0.45
2023–2024	0.33	0.02	0.26	0.29	0.12	0.29	0.41	0.08	0.12	0.26
2024–2025	0.51	0.53	0.57	0.53	0.25	0.44	0.29	0.61	0.13	0.51
Median (m)	0.42	0.43	0.35	0.41	0.40	0.30	0.42	0.64	0.27	

Table 6. Vertical surface change (VCh, $m\,yr^{-1}$) for the two largest glaciers, as median for the three debris-covered glaciers (DC = debris-covered, cf. Table 4), and for two selected rock glaciers (RG). For the location of the landforms, see Fig. 1A.

	Agua Negra Glacier		Glacier ID 71		DC Glaciers (median)		Dos Lenguas RG		El Paso RG	
	VCh	LoD	VCh	LoD	VCh	LoD	VCh	LoD	VCh	LoD
2019–2022	−1.51	±0.02	−0.67	±0.04	−0.09	±0.08	−0.08	±0.04	−0.04	±0.03
2022–2023	−0.59	±0.02	−0.09	±0.02	0.02	±0.01	−0.07	±0.09	0.005	±0.01
2023–2024	−1.85	±0.01	−1.13	±0.05	−0.22	±0.10	−0.04	±0.07	0.03	±0.05
2024–2025	−2.4	±0.04	−0.48	±0.01	0.16	±0.02	−0.03	±0.03	−0.07	±0.05

coded for median horizontal velocity and rock glacier surface area, see Figs. S3 and S4.

Rock glacier velocities are spatially heterogeneously present on the various landform surfaces, Fig. 6. El Paso rock glacier (ID 5) is in its upper part characterized by linear ridges in line with the flow direction that exhibit a faster horizontal velocity than the surrounding rock glacier surface, Fig. 6A. Highest velocities of up to $1.09\,m\,yr^{-1}$, Table 7, are reached in its lower part. Dos Lenguas rock glacier and rock glacier ID 9 are characterized by extensional flow in the upper area and c-shaped ridge and furrow morphologies oriented perpendicular to the direction of flow, commencing in the centre area, Fig. 6B–C. For both, highest velocities of up to $1.38\,m\,yr^{-1}$ (2024–2025, LoD $\pm\,0.64\,m\,yr^{-1}$) and up to $1.17\,m\,yr^{-1}$ (2024–2025, LoD $\pm\,0.95\,m\,yr^{-1}$) are reached in the upper part. The rock glacier with ID 40 is characterized by a lower magnitude of horizontal velocity compared to the other three rock glaciers, Fig. 6D. The different rock glaciers fastest for a specific time period are Dos Lenguas in 2019–2022 and 2024–2025, Table 7, ID 23 in 2022–2023 ($1.16\,m\,yr^{-1}$, LoD $\pm\,0.87\,m\,yr^{-1}$), and ID 40 in 2023–2024, Table 7.

The temporal evolution of rock glacier velocities for the 47 rock glaciers for which we have horizontal velocity data for all time episodes shows unchanged velocities over time, Fig. 7A, independent of rock glacier size and magnitude of velocity. Our quality control for our feature tracking approach, the residue correlation coefficients, indicate higher quality feature tracking for the time periods after 2022 consistent for the three rock glaciers, Fig. 7B–D, representative of all landforms, Fig. S5.

4.4 Comparison of Pléiades- and DGNSS-based vertical and horizontal rock glacier velocities

Vertical and horizontal errors of our DGNSS measurements describe their measurement quality. The magnitude of acceptable error depends on the magnitude of the surface changes investigated. Our DGNSS vertical errors at all three sites (El Paso and Dos Lenguas rock glaciers and Agua Negra Glacial Forefield) range from 0.008 to 0.028 m (2022, median 0.019 m), 0.01 to 0.076 m (2023, median 0.021 m) and 0.009 to 0.041 m (2024, median 0.022 m). Horizontal errors are lower than vertical errors and range from 0.005 to 0.017 m (2022, median 0.009 m), 0.006 to 0.036 m (2023, median 0.012 m), and 0.006 to 0.018 m (2024, median 0.011 m). With very few exceptions on Dos Lenguas rock glacier (2023), all horizontal errors are below $0.02\,m\,yr^{-1}$ and are comparable between the landforms. For a spatial distribution of the errors, see Fig. S6.

Based on the DGNSS measurements, vertical surface changes and horizontal rock glacier velocities are calculated, serving as independent, in situ based validation dataset for the Pléiades-based results, Tables 8 and 9. While vertical surface changes on the El Paso rock glacier surface are positive in median, they are consistently negative for Dos Lenguas rock glacier. Both rock glaciers are characterized by hori-

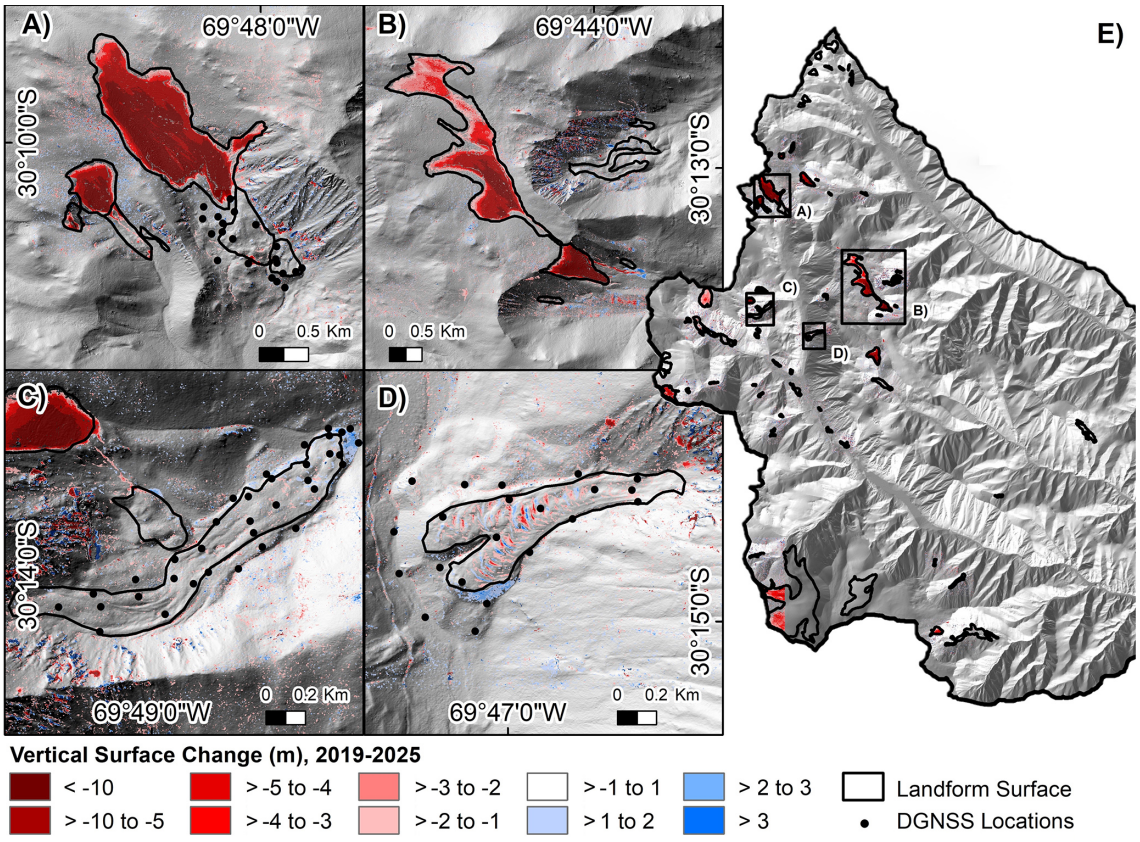

Figure 3. Vertical surface changes (m) between 2019 and 2025, generated by DEM differencing of the co-registered Pléiades DEMs of 2019 and 2025, for Agua Negra Glacier and proximate landforms **(A)**, Glacier ID 71 and proximate landforms **(B)**, El Paso rock glacier and proximate landforms **(C)**, and Dos Lenguas rock glacier **(D)**. For all vertical surface change results, including the locations of panels **(A)** to **(D)**, see panel **(E)**. Polygons based on IANIGLA-CONICET (2018). Colour-scale for vertical surface change applies to all panels. Panels **(A)**, **(C)** and **(D)** include DGNSS locations for repeated measurements, cf. Table 2.

Table 7. Median horizontal velocities ($m\,yr^{-1}$) reached on selected rock glaciers, compared to the median value for all rock glacier surface velocities, cf. Table 4.

	All RG surfaces		El Paso		Dos Lenguas		ID9		ID40	
	HCh	LoD	HCh	LoD	HCh	LoD	HCh	LoD	HCh	LoD
2019–2022	0.28	±0.16	0.64	±0.22	0.86	±0.15	0.57	±0.23	0.44	±0.06
2022–2023	0.64	±0.52	0.97	±0.54	0.92	±0.54	1.03	±0.52	0.64	±0.37
2023–2024	0.46	±0.17	0.95	±0.50	0.98	±0.36	1.18	±0.56	0.56	±0.16
2024–2025	0.82	±0.61	1.09	±0.54	1.38	±0.64	1.17	±0.95	1.23	±0.65
Size	0.05 km^2		0.33 km^2		0.27 km^2		0.24 km^2		0.02 km^2	

zontal velocities of comparable magnitude, particularly considering the effect of LoDs. In all cases, measurements outside the rock glacier surfaces are of much lower magnitude than vertical surface changes and horizontal velocities on the rock glacier surfaces. In Agua Negra Glacial Forefield, the DGNSS measurements indicate vertical and horizontal surface stability with median surface changes close to zero. For a spatial distribution of the DGNSS-based surface changes at all three sites, see Fig. S7.

With the above-presented in situ dataset, we can compare our Pléiades-based surface changes and determine differences between the quantified vertical surface changes and horizontal rock glacier velocities derived using the two datasets, Table 10 and 11. Differences on both rock glacier surfaces and in the Agua Negra Glacial Forefield correspond

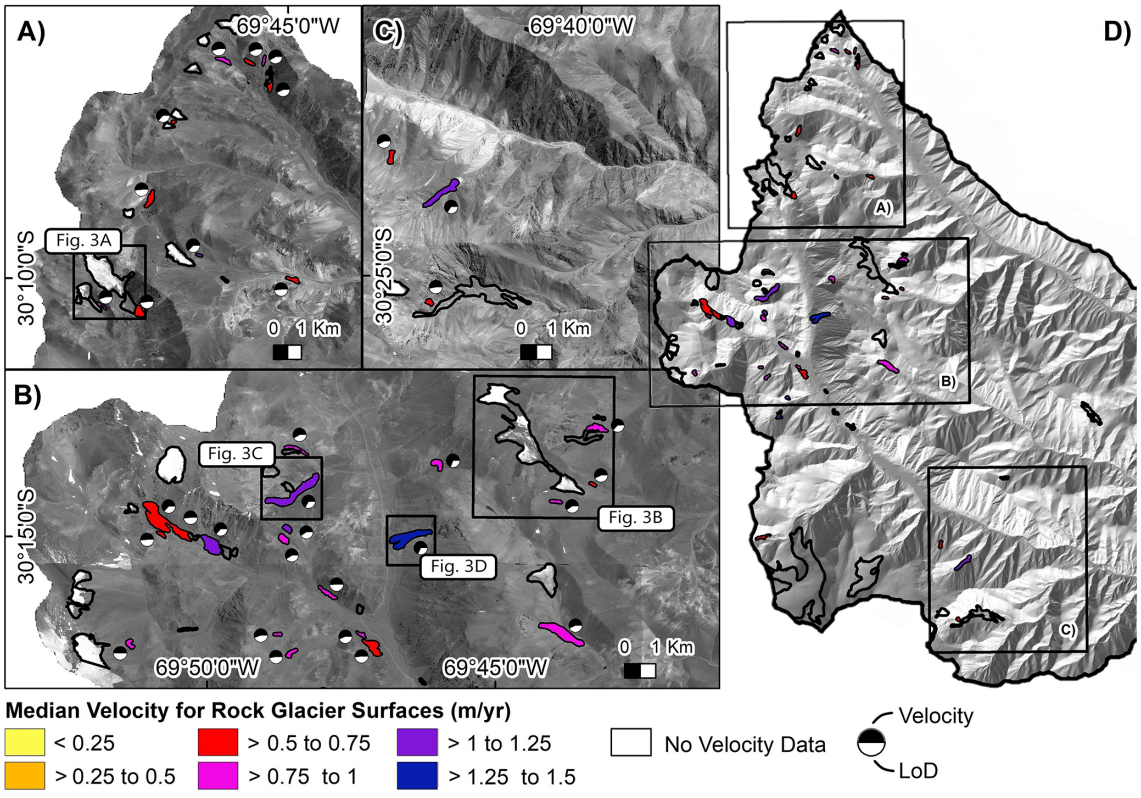

Figure 4. Median velocities ($m\,yr^{-1}$) for rock glacier surfaces between 2019–2025, categorized and normalized to years. (Peri)glacial landforms as mapped by IANIGLA-CONICET (2018), portrayed on top of the Pléiades panchromatic orthophotos for 2024 **(A–C)** and a hillshade based on the 2022 Pléiades imagery **(D)**. Ratios between the horizontal velocity (black) and LoD (white) of each landform are provided as pie charts **(A–C)**. For specific location of the rock glaciers, see panel **(D)**.

Table 8. DGNSS-based vertical surface changes ($m\,yr^{-1}$, median) reached on El Paso and Dos Lenguas rock glaciers (RG), as well as in the Agua Negra Glacial Forefield. LoDs per measurement ($m\,yr^{-1}$) are provided in brackets. For the rock glaciers, surface changes are split in the rock glacier surface and the surrounding terrain, allowing for their separate investigation. Changes are provided for up to two time episodes, depending on the availability of measurements, cf. Table 2.

	El Paso RG		Dos Lenguas RG		Agua Negra Glacial Forefield
	Surface	Not surface	Surface	Not surface	
2022–2023			−0.19 (±0.04)	0 (±0.03)	0 (±0.02)
2023–2024	0.16 (±0.03)	0.3 (±0.03)	−0.21 (±0.04)	0.07 (±0.04)	0.05 (±0.03)

to less than a pixel. Given our feature tracking approach for quantifying horizontal velocities, only DGNSS points within the landform polygon and the 50 m buffer can be compared.

5 Discussion

5.1 Co-registration factors, DEM, and vertical surface change and horizontal velocity quality

The offset between the acquired panchromatic Pléiades imagery is highest in z dimension compared to the x and y dimension, Table 3 and Fig. S2. Linear co-registration shifts calculated over stable terrain excluding the landform surfaces do not exceed ±0.20 m (x) and ±0.59 m (y), Table 3. They indicate relatively good alignment between the panchromatic Pléiades acquisitions in x and y dimension even prior to our co-registration. Co-registration for the z dimension is of higher importance with correction factors up to −1.55 m (2024–2025, tile B) and 2.62 m (2019–2022, tile R), Table 3, respectively. While our shift in z direction is high compared to the x and y component, it is low compared to Rieg et al. (2018) (offsets x, y, z of 4, −3.2, and 4.8 m, Pléiades-based DEMs in ERDAS IMAGINE) and Beraud et al. (2023) (offsets x, y, z of up to −9.89, 7.79, and 12.40 m, Pléiades-

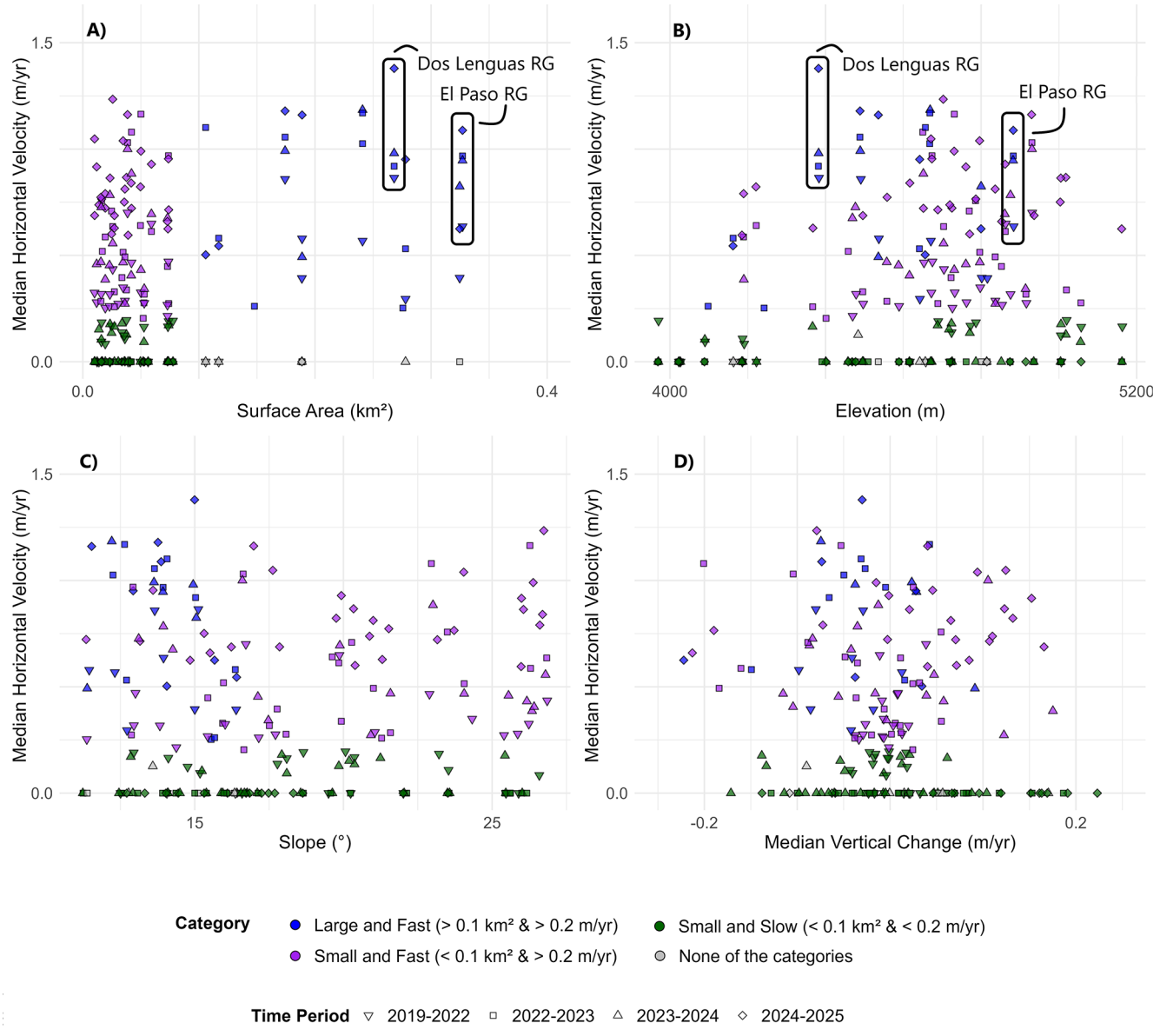

Figure 5. Median velocities for rock glacier surfaces ($m\,yr^{-1}$) and their concurrence with the rock glacier polygon size **(A)**, median elevation **(B)**, median slope **(C)** and median vertical surface change **(D)**, all calculated for the rock glacier surfaces. Elevation and slope are calculated for the beginning of each time period, leading to variability in values and to us refraining from marking Dos Lenguas and El Paso rock glaciers in panels **(C)**–**(D)**. For rock glacier categories and time periods, see legend.

Table 9. DGNSS-based horizontal velocities ($m\,yr^{-1}$, median) reached on El Paso and Dos Lenguas rock glaciers (RG), as well as in the Agua Negra Glacial Forefield. For further specifics, see caption of Table 8.

	El Paso RG		Dos Lenguas RG		Agua Negra Glacial Forefield
	Surface	Not surface	Surface	Not surface	
2022–2023			0.80 (±0.02)	0.04 (±0.04)	0.04 (±0.01)
2023–2024	0.66 (±0.11)	0.07 (±0.11)	1.14 (±0.13)	0.04 (±0.11)	0.07 (±0.01)

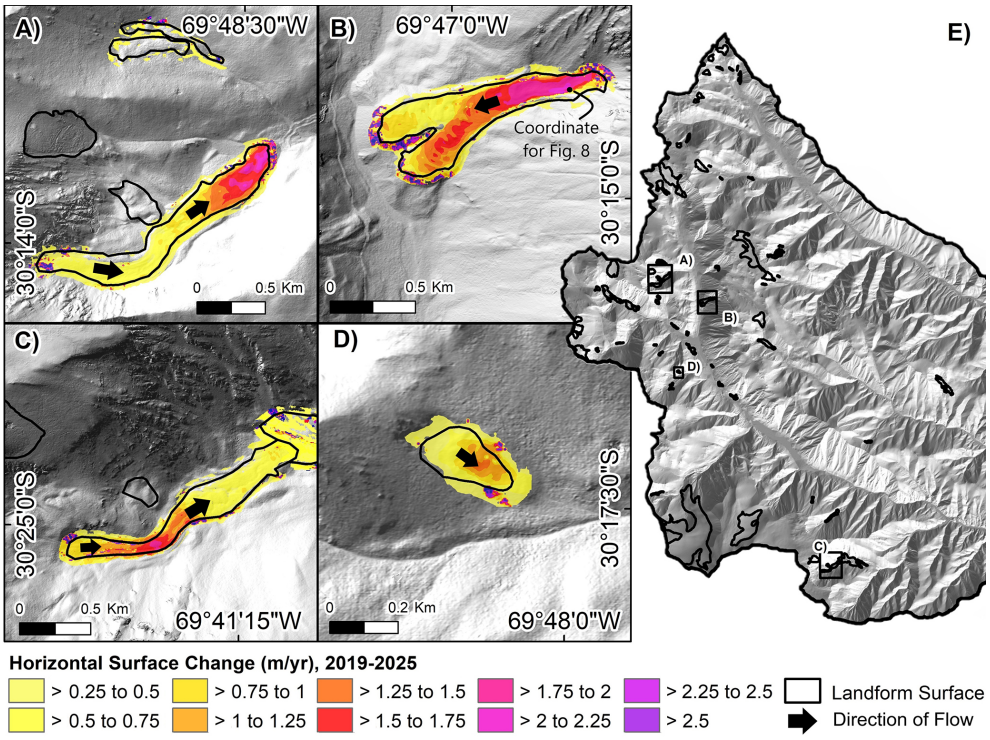

Figure 6. Magnitude and pattern of our Pléiades-based rock glacier surface velocities between 2019 and 2025 ($m\,yr^{-1}$) for El Paso **(A)**, Dos Lenguas **(B)** rock glaciers, as well as the rock glaciers with the IDs 9 **(C)**, and 40 **(D)**. Median rock glacier velocity generated based on our panchromatic Pléiades imagery and tracked on the landforms surface with equally, 5 m spaced points. Consequent velocities at 5 m resolution are shown on a hillshade based on the 2022 Pléiades imagery (cf. Table 1), together with the landform polygons as mapped by IANIGLA-CONICET (2018). Colour-scale for horizontal velocity applies to all panels.

Table 10. Differences between DGNSS- and Pléiades-based vertical surface changes ($m\,yr^{-1}$, median) on El Paso and Dos Lenguas rock glaciers (RG), as well as in the Agua Negra Glacial Forefield.

	El Paso RG		Dos Lenguas RG		Agua Negra Glacial Forefield
	Surface	Not surface	Surface	Not surface	
2022–2023			0.08	0.32	0.00
2023–2024	−0.02	−0.32	0.16	−0.47	−0.18

based DEMs in ASP). As expected, our linear shifts are independent of the targeted location within the catchment, of time, and of the landforms type – supporting the technical rather than geomorphological nature of the need for co-registration. We do not see a difference in the magnitude of the correction factors needed to co-register the stereo dataset (2019), compared to the tri-stereo datasets (2022–2025). Based on the similarity of the 2019–2022 time period to the other time periods, cf. Figs. 2 and 7, we conclude the stereo acquisition to be suitable for vertical and horizontal rock glacier surface change monitoring in the Dry Andes. In comparison, Berthier et al. (2014) conclude a moderate effect of the tristereo benefit, including the reduction of the percentage of data voids.

Artefacts or missing values in our DEMs occur in areas with steep slope. These artefacts are not related to our DEM generation but to the Pléiades data-take which includes no data values for these steep slopes due to mismatches during image correlation. In the Rodeo basin and with our processing approach, we do not see generated spikes in the DEMs as described by Ruiz and Bodin (2015). The number of artefacts in our DEMs is very small. This is mainly due to the vegetation-freeness of the study area as well as the semi-global matching strategy which tend to smooth the surface of the reconstructed DEMs. With a DEM resolution of 1 m, the DEMs used in this study are of higher resolution than used in other studies (Beraud et al., 2023; Falaschi et al., 2023, 2025; Pitte et al., 2022).

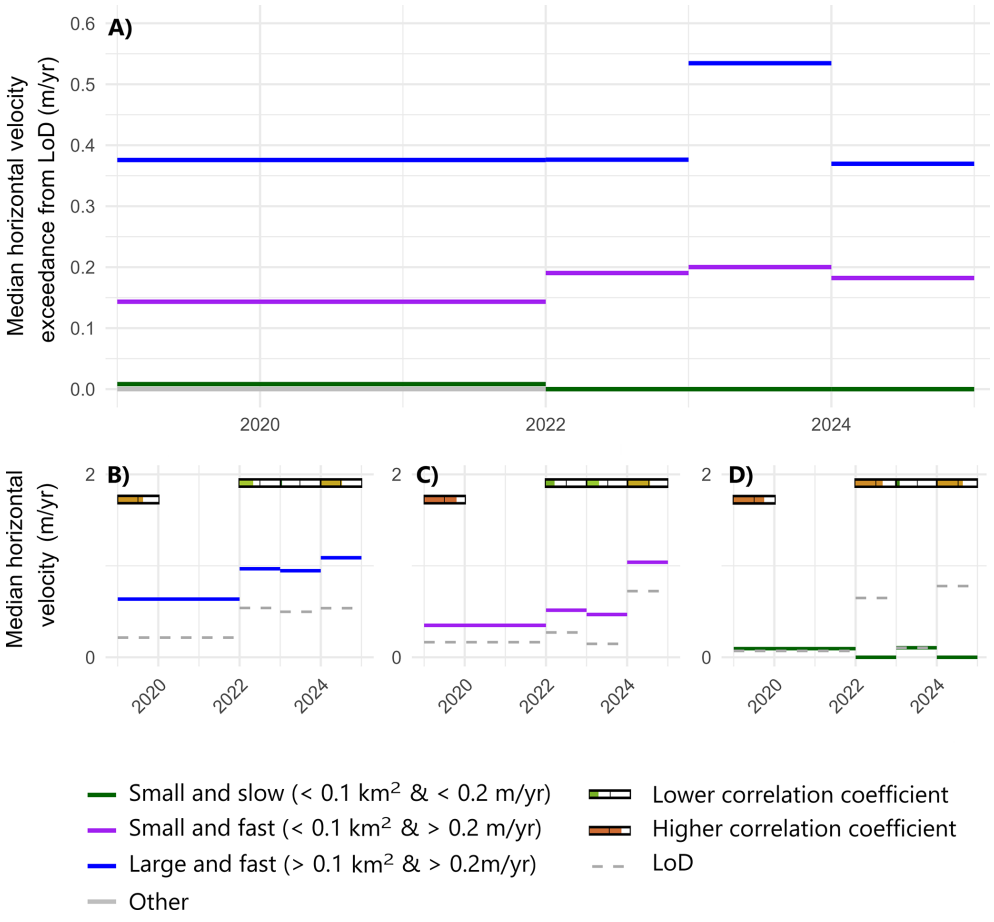

Figure 7. Temporal evolution of median rock glacier surface velocity exceedance from LoD ($m\,yr^{-1}$) between 2019 and 2025 based on feature tracking on panchromatic Pléiades imagery. Median rock glacier velocity is calculated for the rock glacier surface based on tracked horizontal velocity at 5 m resolution. Exceedance is calculated from the corresponding LoD. Rock glaciers are attributed to the three categories when $> 0\,m\,yr^{-1}$ and at all time periods coherent with the respective category **(A)**. Selected rock glaciers and their temporal evolution of velocities over time including their LoD and the quality indication using residue correlation coefficients. The latter are included as bars – one each per time period **(B–D)**. For velocity patterns of all 47 rock glaciers including LoDs and residue correlation coefficients, see Fig. S5.

Table 11. Differences between DGNSS- and Pléiades-based horizontal velocities ($m\,yr^{-1}$, median) on El Paso and Dos Lenguas rock glaciers (RG), as well as in the Agua Negra Glacial Forefield.

	El Paso RG		Dos Lenguas RG		Agua Negra Glacial Forefield
	Surface	Not surface	Surface	Not surface	
2022–2023			−0.01	−0.63	0.01
2023–2024	−0.35	0.03	0.11	0.01	−0.07

Related to our DEM generation workflow, vertical surface change cannot be monitored on all glaciers. This is due to limited heterogeneity of glacier surface characteristics leading to gaps in the DEMs as the photogrammetric processing fails to generate elevation information for these areas, cf. 4.3, Fig. 3E. According to Berthier et al. (2014), the Pléiades imagery's radiometric range (12 bit) limits these effects compared to SPOT1-5 and ASTER. The effect is, however, also encountered by other studies (Beraud et al., 2023; Falaschi et al., 2023).

LoDs calculated as median vertical surface change at 1000 random points in the vicinity of the landforms lead to low LoDs in comparison to the magnitude of vertical surface changes, particularly for glaciers, cf. Table 4. Investigations of vertical surface change of rock glaciers are scarce (Vivero and Lambiel, 2024), particularly for studies using Pléiades

imagery (Falaschi et al., 2025). Thus, a comparison of our LoD calculation with other studies is extremely limited. For rock glacier velocities, all horizontal velocities quantified exceed our LoDs, Figs. 6 and 7. Comparatively low LoDs highlight the stability of surfaces assumed to be stable and support the suitability of panchromatic Pléiades imagery for feature tracking.

Residue correlation coefficients, here used as quality control of the feature tracking approach, cf. 3.5, are in general below 0.5 in median – independent of the respective rock glacier polygon or time period. Their variability between the time periods is higher than between the landforms, highlighting the technical nature of their correlation, cf. Tables 5 and S2. The analysis of residue correlation characterises the time period 2023–2024 as particularly high in quality, not corresponding to the Pléiades tiles with the least co-registration needed, cf. Table 3. Though not fully portrayed in the residue correlation coefficient, we experience the effect of image distortion to be higher on rock glaciers located on steep slopes compared to locations closer to valley bottoms. This corresponds often with smaller landforms, as larger landforms with their elongated tongues "flatten" the topography by building up bodies of rock and ice, cf. Fig. 7D.

While the use of the National Inventory of Glaciers for the landform boundaries allows upscaling our analysis, it restricts the landform surface to a static measure, rather than the surface being adapted for each year. This introduces error on the calculation of median vertical surface changes and horizontal velocities and prevents the potential detection of new landforms. We reduce the impact of the inventory by calculating vertical surface change for bounding boxes with 500 m distance to the landform polygon and with buffered polygon outlines during feature tracking. We highlight the need to display the complex and variable spatial distribution of surface changes within the landform, cf. Figs. 3 and 6, next to the calculated statistics and further agree with Ferri et al. (2020) that highlight the effect of the choice of an inventory, e.g., a national versus a global one.

5.2 Validation of Pléiades-based surface changes with DGNSS data

Difference of our Pléiades-based vertical change to the vertical change measured with the DGNSS equipment is of lowest magnitude for the stable forefield of Agua Negra Glacier, cf. 4.2 and Fig. 3A. Higher difference correlates with a higher magnitude of vertical surface change dynamics at Dos Lenguas and El Paso rock glaciers, cf. 4.2 and Fig. 3C–D. However, difference between the DGNSS measurements and the Pléiades-based vertical surface changes is of lower magnitude for the rock glacier surface compared to the DGNSS measurements located off-site the rock glacier surfaces, cf. 4.2. We hypothesize this difference to be caused by higher vertical accuracies of our DGNSS measurements located at the rock glacier surfaces compared to the surrounding terrain, see Fig. S6 – paired with a very dynamic off-surface environment for El Paso rock glacier, cf. Fig. 3C. Further, we hypothesize the higher accuracies of the DGNSS measurements on the rock glacier surfaces compared to their surroundings to stem from the elevated location on the surface allowing for a good connection between the DGNSS base and rover, compared to the off-surface DGNSS measurement locations partially obscured by the rock glacier body. Similar to the comparison of DGNSS- and Pléiades-derived vertical surface changes, differences between the DGNSS- and Pléiades-derived horizontal velocities are smallest for the Agua Negra Glacier forefield, cf. 4.2, highest for El Paso rock glacier (-0.35 m, 2023–2024) and low in general (all < 1 pixel). The present spatial pattern of differences in magnitude between DGNSS measurements, Fig. S7, is equivalent to our Pléiades-based approach, supporting the feasibility of the method.

5.3 Vertical surface change of glaciers in the Rodeo Basin

Our Pléiades-based vertical surface changes reveal glaciers at higher elevation and of larger size to be less prone to surface lowering, cf. Fig. 2B–C. This is in agreement with the temperature gradient and Al-Yaari et al. (2023) that find small glaciers to be affected by more pronounced loss – supporting the suitability of our approach. We refrain from calculating glacier mass balances given our limited in situ knowledge on glacier ice density. Before comparing our results to the literature, we highlight the effect of glacier surface delineation (cf. 5.1), as also discussed by, e.g., Ferri et al. (2020). The glacier we refer to with ID 71 as mapped by IANIGLA-CONICET (2018), cf. Fig. 3B, is split in two WGMS glacier IDs (32927, 32920). Based on the geodetic method, its mean annual elevation change is attributed values ranging from $-0.2\,\mathrm{m\,yr^{-1}}$ (2000–2012) to -0.5 (2009–2014) for the first WGMS ID and predominantly around $-0.4\,\mathrm{m\,yr^{-1}}$ for different measurement periods between 1999 and 2019 for the second (Dussaillant et al., 2019; Braun et al., 2019; Hugonnet et al., 2021) – contrasting with our Pléiades-based quantification of surface changes, Table 6, due to these differences in delineation.

Pitte et al. (2022) calculate mass balances ranging between -0.79 m w.e. (2014–2025, cumulative for entire glaciological year) and -3.67 m w.e. (2020–2021, see before) for Agua Negra Glacier based on the glaciological method (Cogley et al., 2011). Their annually repeated measurements are all negative and increase in time with one exception (2016–2017), indicating accelerated downwasting in agreement with literature (Dussaillant et al., 2019; Masiokas et al., 2020; Ferri et al., 2020). Based on DEM differencing using, among others, Pléiades-based DEMs, Pitte et al. (2022) report a generalized thinning with high magnitudes at lower elevations which we can attest with our data, cf. Fig. 3A. Pitte et al. (2022) present vertical surface changes of ca. $1\,\mathrm{m\,yr^{-1}}$ between 2013–2019

in the Agua Negra centre and upper parts and changes of ca. $2\,\mathrm{m\,yr^{-1}}$ between 2013 and 2019 in the lower and western parts. This corresponds in magnitude with our vertical change results for Agua Negra Glacier as well as in pattern, Table 6 and Fig. 3A. Pitte et al. (2022) further report a 23 % reduction of the Agua Negra surface area between 1959 to 2019. While not part of this study we highlight the suitability of panchromatic and even multispectral Pléiades imagery to continue the assessment of surface area changes using our Pléiades acquisitions, cf. Table 1. Ayala et al. (2025) estimate a 35 % area loss of the debris-free area of Tapado glacier between 1956 and 2024 located in the neighbouring catchment in Chile – elucidating a similarity of glacier response on both sides of the Andes. In contrast, they observe an increase of the debris-covered area for Tapado glacier which reduces comparability to Agua Negra glacier that does not have a debris-covered part.

5.4 Vertical surface change of debris-covered glaciers in the Rodeo Basin

As expected, given their higher ice content compared to rock glaciers, vertical surface change is higher on the debris-covered glaciers in the Rodeo basin compared to the rock glaciers, Fig. 2A. This is in agreement with Ferri et al. (2020) that find mass balances of higher magnitude for debris-covered glaciers compared to rock glaciers based on the ASTERIX method (Dussaillant et al., 2019) in the Central Andes (30 to 37°). For this study, however, we highlight that the three debris-covered glaciers are too little in number to draw representative conclusions upon their vertical surface change behaviour – particularly on detailed ablation patterns or the development of supraglacial ponds or ice cliffs as conducted, e.g., in Ayala et al. (2025) and Falaschi et al. (2021). Ayala et al. (2016) find similar streamflow contributions of debris-covered glaciers compared to glaciers, highlighting their hydrological significance. This significance contrasts with a strong underrepresentation of studies on debris-covered glaciers in glaciological studies (Masiokas et al., 2020).

Ferri et al. (2020) detect for the Central Andes (30 to 37°) highest mass balance losses for partly debris-covered glaciers, followed by clean ice glaciers and contrasting with completely debris-covered glaciers and rock glaciers characterized by almost zero mass balances (e.g., rock glaciers: $-0.02 \pm 0.19\,\mathrm{m\,w.e.\,yr^{-1}}$, 2000–2018). Aside the partly debris-covered glaciers which we do not address here, this is well reflected in our results, cf. Fig. 2A. It highlights the strong differences in vertical surface change behaviour between the landforms. The question here is the comparability between the meaning of vertical surface changes on glaciers and rock glaciers, which is why we focus on rock glacier horizontal velocities as indicator of the (in)stability of permafrost conditions in the next chapter.

5.5 Rock glacier kinematics in the Rodeo Basin

For Dos Lenguas rock glacier, our Pléiades-based rock glacier vertical surface changes, Table 6, and horizontal velocities, Table 7, are in good agreement with UAV-based rock glacier vertical surface changes and horizontal velocities for Dos Lenguas rock glacier available for 2016-2018 (Halla et al., 2021) and 2016–2024 (Stammler et al., 2025a), both in terms of magnitude, Fig. 8, and pattern. In terms of pattern, highest values of 1.5 to $2\,\mathrm{m\,yr^{-1}}$ are reached in the upper zone, both in Fig. 6B as well as the literature (Halla et al., 2021; Stammler et al., 2025a). Strozzi et al. (2020) quantify horizontal surface velocities ranging between 1.5 and $2\,\mathrm{m\,yr^{-1}}$ (2015–2020) for the upper part of Dos Lenguas rock glacier, based on interferometric synthetic aperture radar (InSAR) and offset tracking. These projected values are in good agreement with our Pléiades-based horizontal velocities, Fig. 8. While we acknowledge the challenges surrounding the comparison of optical and radar imagery-based rock glacier surface change quantification (view angles, different sources of error, different time periods, etc.) and caution a detailed comparison other than the comparison of general magnitude, we highlight the inter-methodological agreement of magnitude between the UAV-, Pléiades-, and InSAR-based investigations.

Except for Dos Lenguas rock glacier, no other rock glaciers in Rodeo basin have been monitored for surface change. This highlights the great benefit of the satelliteborne analysis and its scalability compared to, e.g., UAV-based rock glacier surface change monitoring, as the number of rock glaciers investigated is unprecedented and such comparisons would else not be possible. Median horizonal surface changes for all rock glaciers investigated in this study, Tables 4 and 6, are in agreement in terms of magnitude with average velocities of $0.54 \pm 0.03\,\mathrm{m\,yr^{-1}}$ for rock glaciers in the neighbouring La Laguna catchment (Chile) as detected by Robson et al. (2022). We do not detect a regional trend in increasing rock glacier velocities in the Rodeo basin between 2019 and 2025, Fig. 7. All horizontal velocities quantified with our method remain unchanged within the time period monitored. This absence of such a trend is independent of a rock glaciers' size, median horizontal velocity, elevation, or slope. Apart from the median horizontal velocity exceedance from LoD which facilitates a comparison among the different rock glaciers, Fig. 7B–D as well as Fig. S5 portray the unprecedented strength of the dataset including the median horizontal velocity for each of the rock glaciers for each time period together with the respective LoD and our quality control – the residues' correlation coefficient. A plausible explanation for the absence of a basin-wide acceleration is that, in this semi-arid Andean setting, persistently low precipitation may limit both seasonal snow insulation and liquid-water input into the active layer, thereby damping interannual variability in ground thermal conditions and hydromechanical softening that can otherwise promote speed-ups

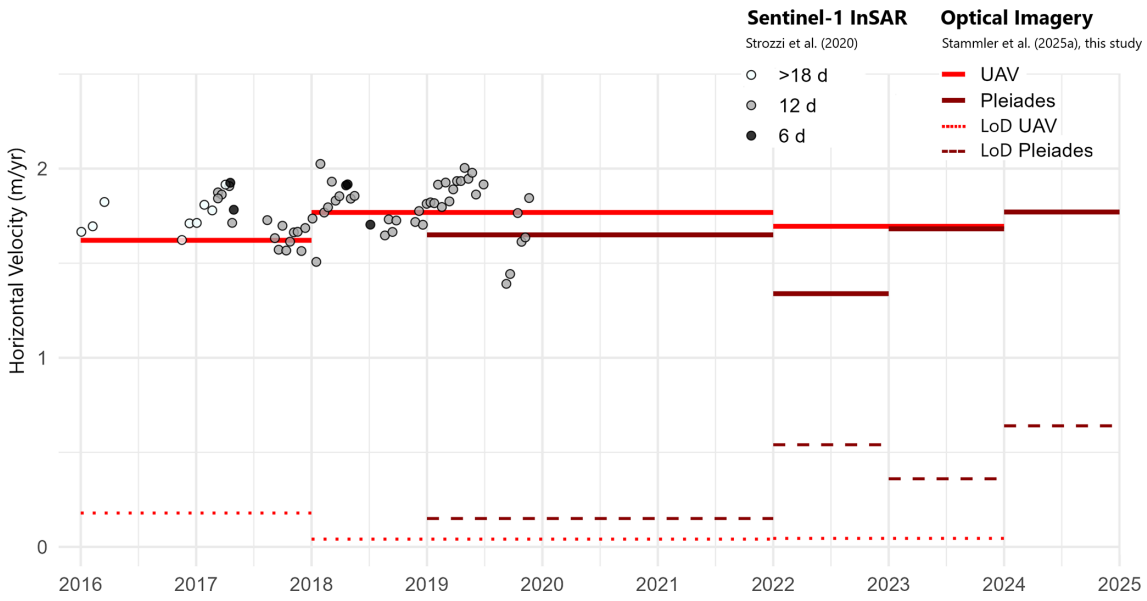

Figure 8. Inter-method comparison between our Pléiades-based rock glacier velocity compared to Sentinel-1 InSAR (Strozzi et al., 2020) and UAV-based rock glacier velocity (Stammler et al., 2025a), all for a coordinate located in the upper part of Dos Lenguas rock glacier, see Fig. 6B. The colour of the dots corresponds to differences in time interval caused by the observation scenarios of the Sentinel-1A and 1B satellites. The InSAR-based velocity is measured along LOS and is projected along the maximum slope direction, for details please see Strozzi et al. (2020). Given this projection, we do not reproject the optically-derived velocities (solid lines, red: UAV, dark red: Pléiades). Dashed lines indicate the corresponding LoDs. Note that horizontal velocities reached in the upper part of Dos Lenguas rock glacier are higher than respective median values.

in rock glacier creep (Cicoira et al., 2019). This interpretation is consistent with evidence that aridity strongly constrains permafrost thermal regimes in the Dry Andes (Koenig et al., 2025) and with recent findings that precipitation scarcity can contribute to comparatively stable rock glacier behaviour (Stammler et al., 2025a). Under this hypothesis, the slightly higher velocities for large rock glaciers in 2023–2024 would reflect short-lived departures from typical moisture limitation (e.g., an anomalously wet season) similar to the variability described in Halla et al. (2021), a possibility that requires confirmation using local precipitation and/or snow proxies and longer kinematic time series.

The lack of a regional trend in increasing velocities determined in this study elucidates stable permafrost conditions in Rodeo basin during 2019–2025. While we acknowledge the limitations of our short monitoring period, we highlight the data scarcity in this region of the world – particularly also for rock glacier monitoring (Hu et al., 2025). The detected lack of a regional trend is in agreement with a longer-term monitoring (1968–2023) by Blöthe et al. (2024) who identify unchanged rock glacier velocities in the Valles Calchaguíes region (24–25° S, Argentinean Andes) and Falaschi et al. (2025) who report a mixed signal of acceleration and deceleration of rock glacier velocities in Central Patagonia (47° S, Argentinean Andes) between 2018 and 2023. It contrasts with findings in the Alps (Kellerer-Pirklbauer et al., 2024; Manchado et al., 2024; Marcer et al., 2021) and North America (Kääb and Røste, 2024). Based on borehole measurements, Koenig et al. (2025) find no clear warming indication for ground temperatures in the Andes (27–34°) – further supporting the implication on permafrost conditions of our quantification of rock glacier velocities. We highlight the strong need for continued monitoring of rock glaciers in this basin in this potentially dynamic point in time.

6 Conclusions

All glaciers in our study area of the Rodeo basin, located in the Dry Andes, are characterized by surface lowering. Agua Negra Glacier stands out with a maximum total surface lowering of −8.99 m (2019–2025). Vertical surface change based on Pléiades DEM differencing confirm smaller glaciers and glaciers at lower altitude to be prone to higher vertical surface lowering. Vertical surface changes on debris-covered glaciers are of a much lesser magnitude compared to glaciers, and of a higher magnitude than rock glaciers. Rock glaciers are characterized by minimal median vertical surface changes with high variability of negative and positive balances in time.

In contrast to the decline in the glacial domain, we do not see a regional trend of increasing rock glacier velocities for 2019–2025. This trend is absent independent of a rock glaciers' size, median horizontal velocity, elevation, or slope. Magnitudes of rock glacier velocities are heterogeneously

present across the basin, with our monitoring for the entire basin allowing for showing fastest creep rates for the rock glaciers with the largest surface areas. Monitoring 47 rock glaciers further highlights that those velocities are heterogeneously present within the landforms, with similar magnitudes of change partially reached in the upper, and partially the lower part of respective landforms.

Both for vertical surface change and horizontal velocities, our validation of the Pléiades-based quantification with repeated DGNSS measurements at three selected sites with in total 78 DGNSS measurements indicate minor differences below one pixel and support the suitability of Pléiades imagery for cryospheric landform monitoring. An inter-method comparison of the rock glacier velocities (Pléiades with UAV and InSAR) further enhances this conclusion. Pléiades imagery comes with the disadvantage of the need for tasking, particularly in areas characterized by data scarcity where archive coverage is poor. Initiatives like the Pléiades Glacier Observatory (Berthier et al., 2024) reduce this barrier by enabling access to selected image pairs and DEMs. Despite the remaining challenge in access, Pléiades imagery provides unseen opportunities specifically in remote areas where (physical) access is challenged. We find both stereo and tristereo acquisitions to be suitable for DEM generation at high resolution and with low error, while panchromatic Pléiades imagery particularly with its independence from colour nuances and changing daylight conditions provides a suitable basis for feature tracking. The possibility to increase the spatial coverage of the surface change monitoring to, e.g., catchment scale along with the benefit of monitoring surface change across landform types enables more interdisciplinary studies in the glaciological, geomorphological and hydrological fields.

Based on our comparison of vertical surface changes in the glacial and periglacial domains of the Rodeo basin and our analysis of rock glacier horizontal velocities, we conclude a delayed response of the permafrost landforms to the increasing temperatures that are declining the glaciers and debris-covered glaciers alike. We further hypothesize that the absence of basin-wide rock glacier acceleration is partly linked to extreme aridity, as persistently low precipitation can reduce snow insulation and liquid-water input to the active layer, damping inter-annual variability in ground thermal conditions and limiting kinematic changes. Given the hydrological significance of all meltwaters, we highlight the strong need for continued monitoring of surface changes in the glacial and periglacial domains, supported by interdisciplinary studies focusing on their potential interaction.

Code and data availability. The Pléiades imagery used in this study are commercial, but programs to facilitate academic access exist. These can be accessed via the CNES/Airbus DS Pléiades archive. The derived vertical surface changes for glaciers, debris-covered glaciers and rock glaciers, the derived rock glacier velocities and the DGNSS measurements are available on PANGAEA at https://doi.org/10.1594/PANGAEA.988303 (Stammler et al., 2026). The repository with the image tracking framework is available on GitHub at https://github.com/SimonEbert/PyImageTrack (Ebert and Rehn, 2026).

Supplement. The supplement related to this article is available online at https://doi.org/10.5194/tc-20-2257-2026-supplement.

Author contributions. MS: conceptualization, funding acquisition, methodology (including methodological development), investigation, writing – initial draft, writing – reviewing and editing; JB: conceptualization, methodology (including methodological development), investigation, software (its provision and development), supervision, writing – reviewing and editing, DC: methodology (including methodological development), investigation, resources (provision of data etc.), software (its provision and development), writing – reviewing and editing, SE: methodology (including methodological development), investigation, software (its provision and development), writing – reviewing and editing, RB: resources (provision of data etc.), writing – reviewing and editing, XB: resources (provision of data etc.), writing – reviewing and editing, LS: funding acquisition, supervision, writing – reviewing and editing.

Competing interests. The contact author has declared that none of the authors has any competing interests.

Disclaimer. Publisher's note: Copernicus Publications remains neutral with regard to jurisdictional claims made in the text, published maps, institutional affiliations, or any other geographical representation in this paper. The authors bear the ultimate responsibility for providing appropriate place names. Views expressed in the text are those of the authors and do not necessarily reflect the views of the publisher.

Acknowledgements. This research is funded by the German Research Foundation (DFG, 461744503). Melanie Stammler further acknowledges funding by the German Scholarship Foundation. The generation of the Pléiades-derived products (DEMs and orthoimages) was performed using Ames Stereo Pipeline software (Beyer et al., 2018) and the GRICAD infrastructure (https://gricad.univ-grenoble-alpes.fr, last access: 15 April 2026), which is supported by Grenoble research communities. We are thankful for the mapping efforts of the National Inventory of Glaciers without which studies like this would not be possible. The authors thank Tamara Köhler, Diana Agostina Ortiz, Fabian Flöck, Philipp Reichartz, Till Wenzel, Manon Cramer, Florian Wester, Kathrin Förster and Gabriele Kraus for their help during fieldwork. We further thank our collaboration partners at IANIGLA-CONICET in Mendoza/Argentina, particularly Fidel Roig and Dario Trombotto Liaudat as well as Cristian Villaroel (CIGEOBIO-CONICET, San Juan/Argentina). Lastly, we thank Tazio Strozzi for sharing their Sentinel-1 InSAR data points.

Financial support. This research has been supported by the Deutsche Forschungsgemeinschaft (grant no. 461744503).

Review statement. This paper was edited by Daniel Farinotti and reviewed by Dominik Amschwand and one anonymous referee.

References

Al-Yaari, A., Condom, T., Junquas, C., Rabatel, A., Ramseyer, V., Sicart, J.-E., Masiokas, M., Cauvy-Fraunié, S., and Dangles, O.: Climate Variability and Glacier Evolution at Selected Sites Across the World: Past Trends and Future Projections, Earth's Future, 11, e2023EF003618, https://doi.org/10.1029/2023EF003618, 2023.

Arenson, L. U., Harrington, J. S., Koenig, C. E. M., and Wainstein, P. A.: Mountain Permafrost Hydrology–A Practical Review Following Studies from the Andes, Geosciences, 12, 48, https://doi.org/10.3390/geosciences12020048, 2022.

ASTRIUM: Pléiades Imagery User Guide, Technical Report, USRPHR-DT-125-SPOT-2.0, 1–106, 2012.

Ayala, A., Pellicciotti, F., MacDonell, S., McPhee, J., Vivero, S., Campos, C., and Egli, P.: Modelling the hydrological response of debris-free and debris-covered glaciers to present climatic conditions in the semiarid Andes of central Chile, Hydrol. Process., 30, 4036–4058, https://doi.org/10.1002/hyp.10971, 2016.

Ayala, Á., Robson, B., Navarro, G., MacDonell, S., Kinnard, C., Vivero, S., Thomas, D., Moreno, F., Yáñez, E., Schaffer, N., Segovia, A., Pętlicki, M., Retamal, F., Schauwecker, S., and Casassa, G.: Monitoring the physical processes driving the mass loss of Tapado Glacier, Dry Andes of Chile, J. Glaciol., 71, e52, https://doi.org/10.1017/jog.2025.24, 2025.

Bagnardi, M., González, P. J., and Hooper, A.: High-resolution digital elevation model from tri-stereo Pleiades-1 satellite imagery for lava flow volume estimates at Fogo Volcano, Geophys. Res. Lett., 43, 6267–6275, https://doi.org/10.1002/2016GL069457, 2016.

Barsch, D.: Permafrost creep and rockglaciers, Permafrost Periglac., 3, 175–188, https://doi.org/10.1002/ppp.3430030303, 1992.

Beraud, L., Cusicanqui, D., Rabatel, A., Brun, F., Vincent, C., and Six, D.: Glacier-wide seasonal and annual geodetic mass balances from Pléiades stereo images: application to the Glacier d'Argentière, French Alps, J. Glaciol., 69, 525–537, https://doi.org/10.1017/jog.2022.79, 2023.

Berthier, E., Vincent, C., Magnússon, E., Gunnlaugsson, Á. Þ., Pitte, P., Le Meur, E., Masiokas, M., Ruiz, L., Pálsson, F., Belart, J. M. C., and Wagnon, P.: Glacier topography and elevation changes derived from Pléiades sub-meter stereo images, The Cryosphere, 8, 2275–2291, https://doi.org/10.5194/tc-8-2275-2014, 2014.

Berthier, E., Lebreton, J., Fontannaz, D., Hosford, S., Belart, J. M.-C., Brun, F., Andreassen, L. M., Menounos, B., and Blondel, C.: The Pléiades Glacier Observatory: high-resolution digital elevation models and ortho-imagery to monitor glacier change, The Cryosphere, 18, 5551–5571, https://doi.org/10.5194/tc-18-5551-2024, 2024.

Beyer, R. A., Alexandrov, O., and McMichael, S.: The Ames Stereo Pipeline: NASA's Open Source Software for Deriving and Processing Terrain Data, Earth and Space Science, 5, 537–548, https://doi.org/10.1029/2018EA000409, 2018.

Blöthe, J. H., Falaschi, D., Vivero, S., and Tadono, T.: Rock Glacier Kinematics in the Valles Calchaquíes Region, Northwestern Argentina, From Multi-Temporal Aerial and Satellite Imagery (1968–2023), Permafrost Periglac., 36, 123–136, https://doi.org/10.1002/ppp.2260, 2024.

Blöthe, J. H., Halla, C., Schwalbe, E., Bottegal, E., Trombotto Liaudat, D., and Schrott, L.: Surface velocity fields of active rock glaciers and ice-debris complexes in the Central Andes of Argentina, Earth Surf. Proc. Land., 46, 504–522, https://doi.org/10.1002/esp.5042, 2021.

Bodin, X., Rojas, F., and Brenning, A.: Status and evolution of the cryosphere in the Andes of Santiago (Chile, 33.5°S.), Geomorphology, 118, 453–464, https://doi.org/10.1016/j.geomorph.2010.02.016, 2010.

Borsdorf, A. and Stadel, C.: Die Anden. Ein geographisches Portrait, Springer, Berlin, Heidelberg, 1–465, ISBN 10 3827424577, ISBN 13 978-3827424570,, 2013.

Braun, M. H., Malz, P., Sommer, C., Farías-Barahona, D., Sauter, T., Casassa, G., Soruco, A., Skvarca, P., and Seehaus, T. C.: Constraining glacier elevation and mass changes in South America, Nat. Clim. Change, 9, 130–136, https://doi.org/10.1038/s41558-018-0375-7, 2019.

Caro, A., Condom, T., Rabatel, A., Champollion, N., García, N., and Saavedra, F.: Hydrological response of Andean catchments to recent glacier mass loss, The Cryosphere, 18, 2487–2507, https://doi.org/10.5194/tc-18-2487-2024, 2024.

Cogley, J. G., Hock, R., Rasmussen, L. A., Arendt, A. A., Bauder, 85 A., Braithwaite, R. J., Jansson, P., Kaser, G., Möller, M., Nicholson, L., and Zemp, M.: Glossary of glacier mass balance and related terms, Paris, France, IHP-VII Technical Documents in Hydrology No. 86, IACS Contribution No. 2, UNESCO-IHP, 1–114, 2011.

Cicoira, A., Beutel, J., Faillettaz, J., Gärtner-Roer, I., and Vieli, A.: Resolving the influence of temperature forcing through heat conduction on rock glacier dynamics: a numerical modelling approach, The Cryosphere, 13, 927–942, https://doi.org/10.5194/tc-13-927-2019, 2019.

Cusicanqui, D., Lacroix, P., Bodin, X., Robson, B. A., Kääb, A., and MacDonell, S.: Detection and reconstruction of rock glacier kinematics over 24 years (2000–2024) from Landsat imagery, The Cryosphere, 19, 2559–2581, https://doi.org/10.5194/tc-19-2559-2025, 2025.

Cusicanqui, D., Bodin, X., Duvillard, P.-A., Schoeneich, P., Revil, A., Assier, A., Berthet, J., Peyron, M., Roudnitska, S., and Rabatel, A.: Glacier, permafrost and thermokarst interactions in Alpine terrain: Insights from seven decades of reconstructed dynamics of the Chauvet glacial and periglacial system (Southern French Alps), Earth Surf. Proc. Land., 48, 2595–2612, https://doi.org/10.1002/esp.5650, 2023.

Dall'Asta, E., Forlani, G., Roncella, R., Santise, M., Diotri, F., and Di Morra Cella, U.: Unmanned Aerial Systems and DSM matching for rock glacier monitoring, ISPRS J. Photogramm., 127, 102–114, https://doi.org/10.1016/j.isprsjprs.2016.10.003, 2017.

Dussaillant, I., Berthier, E., Brun, F., Masiokas, M., Hugonnet, R., Favier, V., Rabatel, A., Pitte, P., and Ruiz, L.: Two decades of

glacier mass loss along the Andes, Nat. Geosci., 12, 802–808, https://doi.org/10.1038/s41561-019-0432-5, 2019.

Ebert, S. and Rehn, L.: PyImageTrack. A Python library implementing feature tracking approaches based on the normalized cross-correlation and least-squares matching for usage on rock glaciers, GitHub [code], https://github.com/SimonEbert/PyImageTrack (last access: 15 April 2026), 2026.

Esper Angillieri, M. Y.: Permafrost distribution map of San Juan Dry Andes (Argentina) based on rock glacier sites, J. S. Am. Earth Sci., 73, 42–49, https://doi.org/10.1016/j.jsames.2016.12.002, 2017.

Falaschi, D., Rivera, A., Lo Vecchio Repetto, A., Moragues, S., Villalba, R., Rastner, P., Zeller, J., and Salcedo, A. P.: Evolution of Surface Characteristics of Three Debris-Covered Glaciers in the Patagonian Andes From 1958 to 2020, Frontiers in Earth Science, 9, 671854, https://doi.org/10.3389/feart.2021.671854, 2021.

Falaschi, D., Bhattacharya, A., Guillet, G., Huang, L., King, O., Mukherjee, K., Rastner, P., Yao, T., and Bolch, T.: Annual to seasonal glacier mass balance in High Mountain Asia derived from Pléiades stereo images: examples from the Pamir and the Tibetan Plateau, The Cryosphere, 17, 5435–5458, https://doi.org/10.5194/tc-17-5435-2023, 2023.

Falaschi, D., Blöthe, J., Berthier, E., Tadono, T., and Villalba, R.: Monitoring recent (2018–2023) glacier and rock glacier changes in Central Patagonia using high-resolution Pléiades and ALOS PRISM satellite data, Frontiers in Earth Science, 13, 1601249, https://doi.org/10.3389/feart.2025.1601249, 2025.

Ferri, L., Dussaillant, I., Zalazar, L., Masiokas, M. H., Ruiz, L., Pitte, P., Gargantini, H., Castro, M., Berthier, E., and Villalba, R.: Ice Mass Loss in the Central Andes of Argentina Between 2000 and 2018 Derived From a New Glacier Inventory and Satellite Stereo-Imagery, Frontiers in Earth Science, 8, 530997, https://doi.org/10.3389/feart.2020.530997, 2020.

Fleischer, F., Haas, F., Piermattei, L., Pfeiffer, M., Heckmann, T., Altmann, M., Rom, J., Stark, M., Wimmer, M. H., Pfeifer, N., and Becht, M.: Multi-decadal (1953–2017) rock glacier kinematics analysed by high-resolution topographic data in the upper Kaunertal, Austria, The Cryosphere, 15, 5345–5369, https://doi.org/10.5194/tc-15-5345-2021, 2021.

Gruber, S.: Derivation and analysis of a high-resolution estimate of global permafrost zonation, The Cryosphere, 6, 221–233, https://doi.org/10.5194/tc-6-221-2012, 2012.

Halla, C., Blöthe, J. H., Tapia Baldis, C., Trombotto Liaudat, D., Hilbich, C., Hauck, C., and Schrott, L.: Ice content and interannual water storage changes of an active rock glacier in the dry Andes of Argentina, The Cryosphere, 15, 1187–1213, https://doi.org/10.5194/tc-15-1187-2021, 2021.

Hu, Y., Arenson, L. U., Barboux, C., Bodin, X., Cicoira, A., Delaloye, R., Gärtner-Roer, I., Kääb, A., Kellerer-Pirklbauer, A., Lambiel, C., Liu, L., Pellet, C., Rouyet, L., Schoeneich, P., Seier, G., and Strozzi, T.: Rock Glacier Velocity: An Essential Climate Variable Quantity for Permafrost, Rev. Geophys., 63, https://doi.org/10.1029/2024RG000847, 2025.

Hugonnet, R., McNabb, R., Berthier, E., Menounos, B., Nuth, C., Girod, L., Farinotti, D., Huss, M., Dussaillant, I., Brun, F., and Kääb, A.: Accelerated global glacier mass loss in the early twenty-first century, Nature, 592, 726–731, https://doi.org/10.1038/s41586-021-03436-z, 2021.

IANIGLA-CONICET: ANIGLA – Inventario Nacional de Glaciares y Ambiente Periglacial: Informe de la subcuenca del río Blanco, Cuenca del río San Juan, Technical Report, 2018 (in Spanish).

Kääb, A. and Røste, J.: Rock glaciers across the United States predominantly accelerate coincident with rise in air temperatures, Nat. Commun., 15, 7581, https://doi.org/10.1038/s41467-024-52093-z, 2024.

Kellerer-Pirklbauer, A., Bodin, X., Delaloye, R., Lambiel, C., Gärtner-Roer, I., and Bonnefoy-Demongeot, M.: Acceleration and interannual variability of creep rates in mountain permafrost landforms (rock glacier velocities) in the European Alps in 1995–2022, Environ. Res. Lett., 19, 34022, https://doi.org/10.1088/1748-9326/ad25a4, 2024.

Koenig, C. E. M., Hilbich, C., Hauck, C., Arenson, L. U., and Wainstein, P.: Thermal state of permafrost in the Central Andes (27–34° S), The Cryosphere, 19, 2653–2676, https://doi.org/10.5194/tc-19-2653-2025, 2025.

Köhler, T., Schoch-Baumann, A., Bell, R., Buckel, J., Ortiz, D. A., Trombotto Liaudat, D., and Schrott, L.: Expanding cryospheric landform inventories – quantitative approaches for underestimated periglacial block- and talus slopes in the Dry Andes of Argentina, Frontiers in Earth Science, 13, 1534410, https://doi.org/10.3389/feart.2025.1534410, 2025.

Lenzano, M. G., Lenzano, L., Barón, J., Lannutti, E., Durand, M., and Trombotto Liaudat, D.: Thinning of the Horcones inferior debris-covered glacier, derived from five ablation seasons by semi-continuous GNSS geodetic surveys (Mt. Aconcagua, Argentina), Andean Geol., 43, 47–59, https://doi.org/10.5027/andgeoV43n1-a03, 2016.

Lliboutry, L., Williams, R., and Ferrigno, J. G.: Glaciers of Chilie and Argentina, Geological Survey professional paper, 1386-I-6, Washington, 1998.

Manchado, A. M.-T., Allen, S., Cicoira, A., Wiesmann, S., Haller, R., and Stoffel, M.: 100 years of monitoring in the Swiss National Park reveals overall decreasing rock glacier velocities, Communications Earth & Environment, 5, https://doi.org/10.1038/s43247-024-01302-0, 2024.

Marcer, M., Cicoira, A., Cusicanqui, D., Bodin, X., Echelard, T., and Obregon, R.: Rock glaciers throughout the French Alps accelerated and destabilised since 1990 as air temperatures increased, Communications Earth & Environment, 2, 81, https://doi.org/10.1038/s43247-021-00150-6, 2021.

Masiokas, M. H., Rabatel, A., Rivera, A., Ruiz, L., Pitte, P., Ceballos, J. L., Barcaza, G., Soruco, A., Bown, F., Berthier, E., Dussaillant, I., and MacDonell, S.: A Review of the Current State and Recent Changes of the Andean Cryosphere, Frontiers in Earth Science, 8, https://doi.org/10.3389/feart.2020.00099, 2020.

Nuth, C. and Kääb, A.: Co-registration and bias corrections of satellite elevation data sets for quantifying glacier thickness change, The Cryosphere, 5, 271–290, https://doi.org/10.5194/tc-5-271-2011, 2011.

Pabón-Caicedo, J. D., Arias, P. A., Carril, A. F., Espinoza, J. C., Borrel, L. F., Goubanova, K., Lavado-Casimiro, W., Masiokas, M., Solman, S., and Villalba, R.: Observed and Projected Hydroclimate Changes in the Andes, Frontiers in Earth Science, 8, https://doi.org/10.3389/feart.2020.00061, 2020.

Pitte, P., Masiokas, M., Gargantini, H., Ruiz, L., Berthier, E., Ferri Hidalgo, L., Zalazar, L., Dussaillant, I., Viale, M., Zorzut, V.,

Corvalán, E., Scarpa, J. P., Costa, G., and Villalba, R.: Recent mass-balance changes of Agua Negra glacier (30° S) in the Desert Andes of Argentina, J. Glaciol., 68, 1197–1209, https://doi.org/10.1017/jog.2022.22, 2022.

Réveillet, M., MacDonell, S., Gascoin, S., Kinnard, C., Lhermitte, S., and Schaffer, N.: Impact of forcing on sublimation simulations for a high mountain catchment in the semiarid Andes, The Cryosphere, 14, 147–163, https://doi.org/10.5194/tc-14-147-2020, 2020.

RGIK: Rock Glacier Velocity as an associated parameter of ECV Permafrost: Baseline Concepts, IPA Action Group Rock glacier inventories and kinematics, Technical Report, 12 pp., 2023.

RGIK: IPA Action Group: Rock glacier inventories and kinematics: 22 Newsletter (04.02.3022): Rock glacier velocity as an associated parameter of ECV Permafrost, https://www.unifr.ch/geo/geomorphology/en/research/ipa-action-group-rock-glacier/ (last access: 30 June 2023), 2022.

Rieg, L., Klug, C., Nicholson, L., and Sailer, R.: Pléiades Tri-Stereo Data for Glacier Investigations–Examples from the European Alps and the Khumbu Himal, Remote Sensing, 10, 1563, https://doi.org/10.3390/rs10101563, 2018.

Robson, B. A., MacDonell, S., Ayala, Á., Bolch, T., Nielsen, P. R., and Vivero, S.: Glacier and rock glacier changes since the 1950s in the La Laguna catchment, Chile, The Cryosphere, 16, 647–665, https://doi.org/10.5194/tc-16-647-2022, 2022.

Ruiz, L. and Bodin, X.: Analysis and improvement of surface representativeness of high resolution Pléiades DEMs: Examples from glaciers and rock glaciers in two areas of the Andes, in: Geomorphometry for Geosciences, edited by: Jasiewicz, J., Zwoliński, Zb., Mitasova, H., Hengl, T., Geomorphometry.org, 223–226, https://doi.org/10.13140/RG.2.1.4328.2963, 2015.

Schrott, L.: Die Solarstrahlung als steuernder Faktor im Geosystem der subtropischen semiariden Hochanden (Agua Negra, San Juan, Argentinien), Heidelberger Geographische Arbeiten, 94, ISBN 978-3-88570-094-4, 1994.

Schrott, L.: Some geomorphological-hydrological aspects of rock glaciers in the Andes (San Juan, Argentina), Z. Geomorphol., Supplementband, 104, 161–173, 1996.

Schrott, L. and Götz, J.: The periglacial environment in the semiarid and arid Andes of Argentina - hydological significance and research frontiers, in: Forschen im Gebirge/Investigating the mountains/investigando las Montanas, 53–63, ISBN 978-3-7001-7461-5, 2013.

Schwalbe, E. and Maas, H.-G.: The determination of high-resolution spatio-temporal glacier motion fields from time-lapse sequences, Earth Surf. Dynam., 5, 861–879, https://doi.org/10.5194/esurf-5-861-2017, 2017.

Shean, D. E., Alexandrov, O., Moratto, Z. M., Smith, B. E., Joughin, I. R., Porter, C., and Morin, P.: An automated, open-source pipeline for mass production of digital elevation models (DEMs) from very-high-resolution commercial stereo satellite imagery, ISPRS J. Photogramm., 116, 101–117, https://doi.org/10.1016/j.isprsjprs.2016.03.012, 2016.

Stammler, M., Cusicanqui, D., Bell, R., Robson, B., Bodin, X., Blöthe, J., and Schrott, L.: Vertical surface change signals of rock glaciers: combining UAV and Pléiades imagery (Agua Negra, Argentina), in: Proceedings of the 12th International Conference on Permafrost, Whitehorse Yukon, Canada, 16–20 June 2024, https://doi.org/10.52381/ICOP2024.138.1, 2024.

Stammler, M., Blöthe, J., Flöck, F., Bell, R., and Schrott, L.: Dos Lenguas rock glacier kinematics stable despite warming trend (2016–2024): Surface changes and the role of topography and climate in the Dry Andes of Argentina, Earth Surf. Process. Land., 50, https://doi.org/10.1002/esp.70151, 2025a.

Stammler, M., Blöthe, J., Flöck, F., Bell, R., and Schrott, L.: UAV-based optical imagery, digital elevation models and hillshades of Dos Lenguas rock glacier/Argentinean Dry Andes (30° S, 69° W; 2016, 2018, 2022, 2024) and daily static optical imagery (2023–2024), PANGAEA [data set], https://doi.org/10.1594/PANGAEA.979876, 2025b.

Stammler, M., Blöthe, J., Cusicanqui, D., Ebert, S., Bell, R., Bodin, X., and Schrott, L.: Pléiades imagery based digital elevation models and quantified surface change for (debris-covered) glaciers and rock glaciers in the Dry Andes of Argentina (30° S, 69° W; 2019, 2022, 2023, 2024, 2025), PANGAEA [data set], https://doi.org/10.1594/PANGAEA.988303, 2026.

Strozzi, T., Caduff, R., Jones, N., Barboux, C., Delaloye, R., Bodin, X., Kääb, A., Mätzler, E., and Schrott, L.: Monitoring Rock Glacier Kinematics with Satellite Synthetic Aperture Radar, Remote Sensing, 12, 559, https://doi.org/10.3390/rs12030559, 2020.

Villarroel, C., Tamburini Beliveau, G., Forte, A., Monserrat, O., and Morvillo, M.: DInSAR for a Regional Inventory of Active Rock Glaciers in the Dry Andes Mountains of Argentina and Chile with Sentinel-1 Data, Remote Sensing, 10, 1588, https://doi.org/10.3390/rs10101588, 2018.

Villarroel, C. D. and Forte, A. P.: Spatial distribution of active and inactive rock glaciers and protalus ramparts in a sector of the Central Andes of Argentina, Geographical Research Letters, 46, 141–158, https://doi.org/10.18172/cig.4272, 2020.

Villarroel, C. D., Ortiz, D. A., Forte, A. P., Tamburini Beliveau, G., Ponce, D., Imhof, A., and López, A.: Internal structure of a large, complex rock glacier and its significance in hydrological and dynamic behavior: A case study in the semi-arid Andes of Argentina, Permafrost Periglac., 33, 78–95, https://doi.org/10.1002/ppp.2132, 2022.

Vivero, S. and Lambiel, C.: Annual surface elevation changes of rock glaciers and their geomorphological significance: Examples from the Swiss Alps, Geomorphology, 467, 109487, https://doi.org/10.1016/j.geomorph.2024.109487, 2024.

Zalazar, L. V., Ferri Hidalgo, L., Castro, M. A., Gargantini, H., Giménez, M. M., Pitte, P. M., Ruiz, L. E., and Villalba, R.: Glaciares de Argentina: Resultados preliminares del Inventario Nacional de Glaciares, Revista de Glaciares y Ecosistemas de Montaña, 2, 13–22, 2017.

Zalazar, L., Ferri, L., Castro, M., Gargantini, H., Gimenez, M., Pitte, P., Ruiz, L., Masiokas, M., Costa, G., and Villalba, R.: Spatial distribution and characteristics of Andean ice masses in Argentina: results from the first National Glacier Inventory, J. Glaciol., 66, 938–949, https://doi.org/10.1017/jog.2020.55, 2020.